Risk of Hip Dislocation After LUMiC Reconstruction

the impact of center of rotation

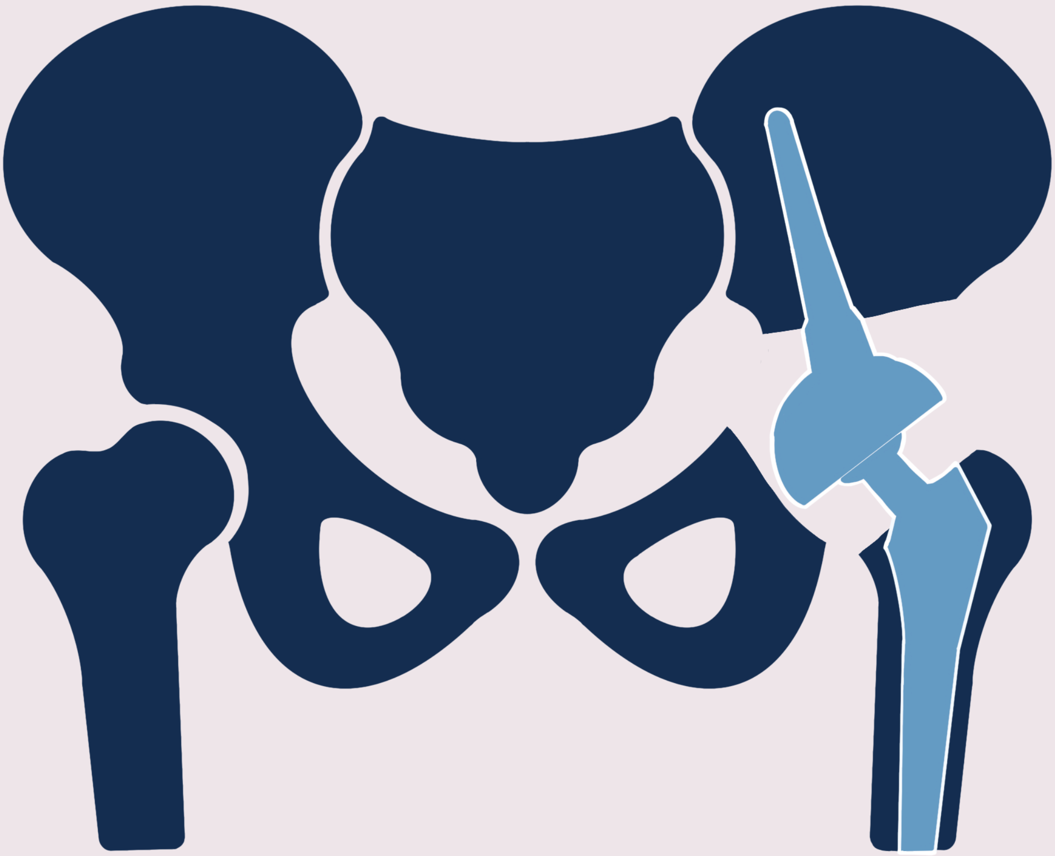

MSc Thesis Technical Medicine

Julia van der Geest

The impact of center of rotation changes on dislocation risk after periacetabular tumor resection and reconstruction using the LUMiC® prosthesis

Julia van der Geest

Student number: 5082676

August 29, 2025

Thesis in partial fulfilment of the requirements for the joint degree of Master of Science in

Technical Medicine

Leiden University - Delft University of Technology - Erasmus University Rotterdam

Master thesis project (TM30004 - 35 ECTS)

Department of Orthopaedics, Leiden University Medical Center

April 2025 – August 2025

Supervisors

Dr.ir. B.L. Kaptein	Technical supervision
Dr. R.E. Evenhuis	Medical supervision

Thesis committee members

Dr.ir. B.L. Kaptein	Leiden University Medical Center (chair)
Dr. R.E. Evenhuis	Leiden University Medical Center
Dr. P.K. Bos	Erasmus Medical Center Rotterdam

An electronic version of this thesis is available at http://repository.tudelft.nl.

Preface

Orthopedic oncology poses complex surgical challenges, especially in the reconstruction of the pelvis after tumor resection. One of the prosthetic solutions used in these cases is the LUMiC prosthesis: a modular system designed to provide stability in difficult anatomical situations. Despite its design, many patients experience hip dislocation postoperatively. It remains unclear which factors contribute most to this risk. One hypothesis is that the position of the center of rotation plays a key role.

In February 2024, I started a 10-week internship as part of the second year of my master's program. During this period, I analyzed data from ten patients treated with a LUMiC prosthesis. It quickly became clear that the topic had much more to offer. With just ten patients, it wasn't possible to draw firm conclusions about dislocation risk. Yet I wanted to find an answer and asked to continue the project. What began as a short internship gradually developed into the subject of this graduation thesis.

I would like to thank my supervisors, Bart and Richard, for their continuous support. Bart, thank you for your excellent guidance, all the meetings and your technical insights that consistently helped move the research forward. Richard, although working from Alrijne Ziekenhuis, you remained closely involved throughout the project. Thank you for your clinical perspective, for connecting me with external centers and for always being willing to think along and provide feedback. Also a special thanks to Marta Fiocco for your help with the statistical analysis.

Thanks also to the D1 researchers and students for the lunch breaks, talks about our projects and for bringing some light into our windowless office. Special thanks to Hilde and Lisa for their support whenever I had questions. I am very grateful to all the orthopedic surgeons, A(N)IOS, cast technicians and nurse practitioners who welcomed me into surgeries and consultations, always taking the time to explain. In particular, I would like to thank Demien for allowing me to observe LUMiC surgeries and sharing your expertise; Jasper for your enthusiastic technical-clinical perspective, help with data export from UMCG and involving me in Brainlab plannings; and Lotje for the many hours spent together in the clinic and casting room. It's been an incredibly valuable and educational experience.

Julia van der Geest
Leiden, August 2025

Abstract

Background and objectives

The LUMiC prosthesis reconstructs periacetabular defects after tumor resection. However, dislocation remains a substantial risk. Alterations in the center of rotation (COR), anteversion (AV) and inclination (INCL) may contribute, but their impact in LUMiC reconstructions has not been studied. This study aimed to assess whether deviations in COR, AV and INCL are associated with dislocation risk.

Methods

An international multicenter retrospective cohort study was conducted in patients who underwent internal hemipelvectomy with LUMiC reconstruction between 2008 and 2022. Changes in preoperative and postoperative COR, AV and INCL were calculated using a semi-automatic method based on 3D models generated from CT data. An univariate Cox regression model was estimated to assess associations with dislocation risk.

Results

Of 114 eligible patients, 60 had postoperative CT scans suitable for analysis. Mean postoperative changes were +9.0 ± 13.7° in AV, -14.1 ± 15.6° in INCL and COR displacement of 4.7 ± 13.7 mm (lateral), 0.7 ± 14.7 mm (anterior), and 16.0 ± 16.2 mm (superior). Dislocation occurred in 11 patients (18.3%). Medial COR displacement was significantly associated with dislocation risk (HR 1.07 per mm; $p = 0.018$), while AV, INCL and other COR components were not.

Conclusion

Medial displacement of the COR after LUMiC reconstruction might increase the dislocation risk. Restoring lateral offset may improve postoperative stability.

List of Abbreviations

2D	Two dimensional
3D	Three dimensional
AP	Anteroposterior (direction)
APP	Anterior pelvic plane
ASA	American Society of Anaesthesiologists
ASIS	Anterior superior iliac spine
AV	Anteversion
BMI	Body mass index
COR	Center of rotation
CT	Computed tomography
HR	Hazard ratio
ICC	Intraclass correlation coefficient
INCL	Inclination
IQR	Interquartile range
ML	Mediolateral (direction)
MSP	Mid-sagittal plane
PT	Pubic tubercles
ROM	Range of motion
SC	Sacral crest
SD	Standard deviation
SI	Superoinferior (direction)

Table of Contents

1

General Background

1.1 Anatomy and function of the pelvis

The pelvis is a complex bony structure composed of the ilium, ischium, pubis and sacrum (Figure 1.1). Together, these elements form a rigid ring that connects the spine to the lower limbs. Two major joints are involved in pelvic function: 1) the hip joint, a ball-and-socket articulation between the femoral head and the acetabulum and 2) the sacroiliac joint, which links the sacrum to the iliac bones. These joints facilitate mobility while providing the necessary stability (1).

The pelvis plays a critical role in weight transmission from the axial skeleton to the lower extremities during standing, walking and running. It also contributes to shock absorption and balance. Therefore, any structural alteration of the pelvis, such as caused by tumor resection, can significantly impact stability, mobility and quality of life (2).

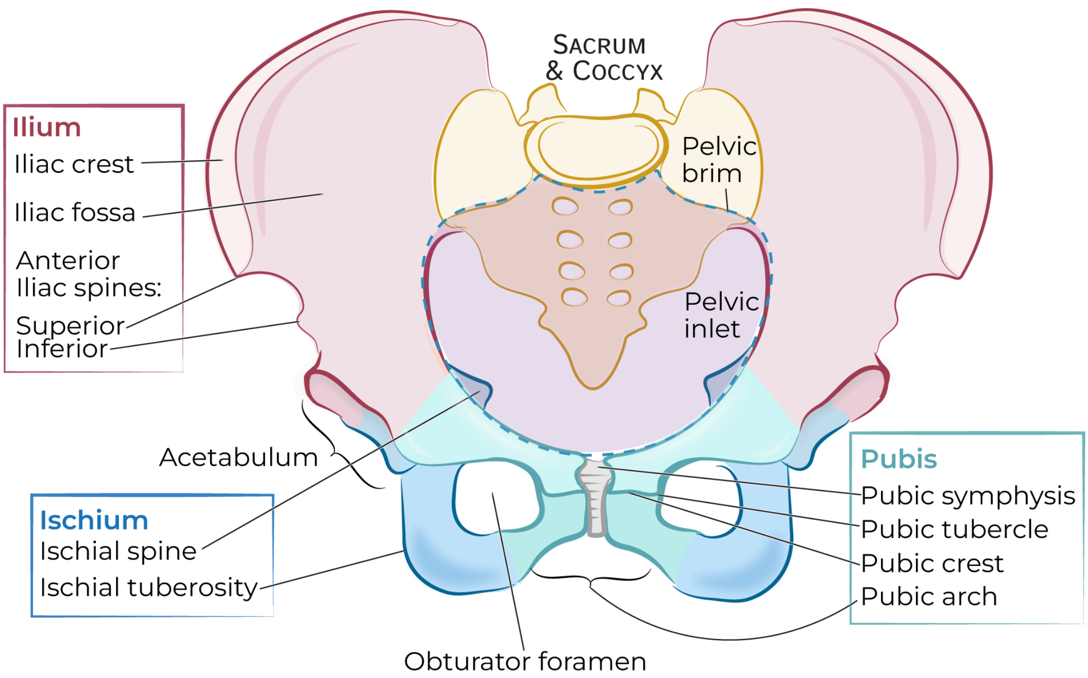

Figure 1.1. Anatomy of the pelvis, showing major bony structures including the ilium, ischium, pubis, sacrum, acetabulum (3).

1.2 Pathology of pelvic bone tumors

Primary bone sarcomas are relatively rare, accounting for approximately 0.2% of all cancer cases, with an incidence of about 0.85 cases per 100,000 individuals per year, equating to roughly 195 new cases annually in the Netherlands (4). Of these, 16% are located in the pelvis (5).

Among primary bone sarcomas, chondrosarcomas are the most common type in adults, with a median age at diagnosis ranging from 30 to 60 years. Osteosarcomas are the most frequent overall and show a bimodal age distribution, with a higher incidence in adolescents and a second peak in individuals aged 70-80. Ewing sarcomas primarily affect children and adolescents, with a median age at diagnosis of 15 years (6).

Bone metastases are far more common than primary bone tumors. The skeleton is the most frequent site of metastasis and approximately 70% of patients who die from cancer have evidence of bone metastases at autopsy (7). These metastases most commonly originate from breast, lung and kidney cancers (8). Treatment depends on the severity and location of bone destruction and is often necessary to prevent pathological fractures, maintain mobility and reduce pain (9,10).

Diagnosis of both primary bone tumors and metastases typically begins with imaging: conventional radiography followed by MRI and when necessary CT. Definitive diagnosis often requires biopsy (11).

1.3 Tumor resection

Pelvic bone tumors pose significant diagnostic and therapeutic challenges due to their anatomical location near critical structures such as major blood vessels, nerves and (pelvic) organs. This proximity, along with tumor size and pelvic anatomy, often makes it difficult to achieve adequate surgical margins (12,13).

Historically, hindquarter amputations were considered the standard treatment for malignant pelvic tumors. However, this procedure is associated with substantial cosmetic, functional and psychological burden (14).

A key development in the surgical management of pelvic tumors occurred in the 1980s with a shift towards limb-salvage procedures, as categorized by Enneking (15). This system divides pelvic resections into four types (I–IV) based on tumor location:

- Type I - Ilium
- Type II - Periacetabular region
- Type III - Pubis and ischium
- Type IV - Sacrum

Bus et al. developed a modified Enneking classification, in which the ilium is split into subtypes IA and IB (Figure 1.2) (16).

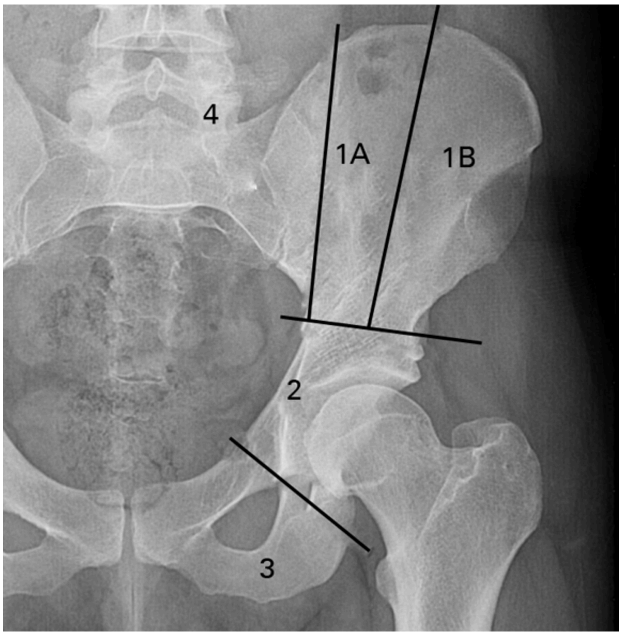

Figure 1.2. Modified Enneking Classification (16)

Pelvic tumor resection is indicated to achieve local tumor control or to prevent structural collapse. These procedures frequently result in large bony defects that require complex reconstruction, which is challenging due to the often massive extent of bone and soft tissue removal, exposing the reconstruction to high biomechanical stresses (16). Reconstructive options include 3D-printed custom made implants for a precise anatomical fit, vascularized fibular grafts providing viable biological support and the "ice cream cone" prosthesis, first introduced by the Birmingham group in 2003 as a modular solution for periacetabular defects (13,17,18). Despite these treatment options, pelvic resections and reconstructions remain associated with high rates of complications, implant failure and even mortality (19,20)

1.4 LUMiC prosthesis

The LUMiC® prosthesis (Implantcast, Buxtehude, Germany), introduced in 2008 to reduce the risk of complications, is a modular pedestal cup system specifically engineered for complex periacetabular reconstructions following tumor resection or major acetabular bone loss (21). The prosthesis allows for relatively straightforward and durable fixation in a biomechanically demanding environment.

The LUMiC system is anchored within the iliac wing, permitting effective fixation even when only the medial ilium remains intact (21). The prosthesis consists of two main components: a stem and an acetabular cup (Figure 1.3). The stem is available in various sizes and lengths and can be implanted either as an uncemented hydroxyapatite (HA)-coated titanium alloy (TiAl6V4) component or as a cemented matt-finished cobalt chromium molybdenum alloy (CoCrMo) version. The acetabular cup, also available in multiple sizes, can be rotated around the implanted stem to fine-tune cup orientation intraoperatively, optimizing hip range of motion and stability. The junction between the stem and cup incorporates sawteeth, which enables secure rotational adjustments before final fixation. Various insert options are available, including dual-mobility liners which might reduce dislocation risk (22).

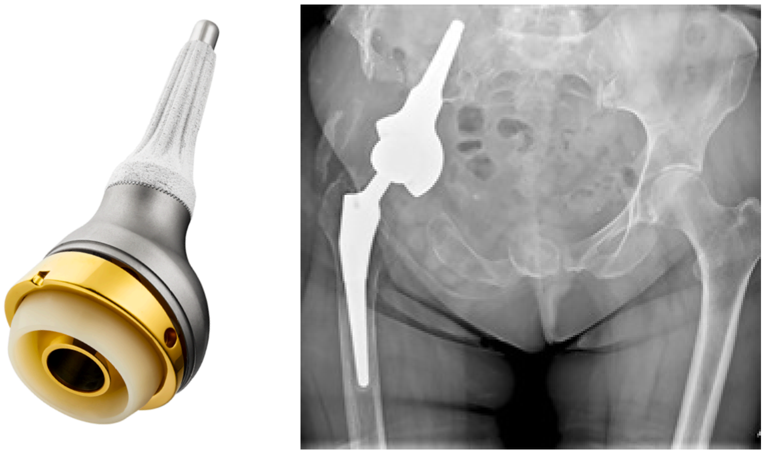

Figure 1.3. Representation of the LUMiC prosthesis. (22,23)

Indications for the LUMiC prosthesis primarily include partial or complete acetabular reconstruction following oncologic resection, complex revision arthroplasty with severe bone loss and situations where conventional fixation options are inadequate.

1.5 Complications

Unfortunately, complications are common with the LUMiC prosthesis. These complications are classified according to the Henderson classification of failure after limb salvage surgery for bone tumors (24), with dislocation (type 1A) and infection (type 4) being the most frequent .

In literature, infection is reported as the most common complication, with rates ranging from 25% to 50%. Dislocation is the most frequently reported mechanical failure, occurring in 19% to 31% of cases (21,25,26).

1.6 Prosthesis position analysis

The positioning of hip prosthesis plays a critical role in the outcome of pelvic reconstructions, particularly after periacetabular tumor resections. Proper orientation of the acetabular component directly affects range of motion (ROM), joint stability, muscle strength, implant wear and the risk of dislocation (27–33). Key parameters to describe prosthetic orientation include the hip center of rotation, anteversion and inclination. Displacement of the center of rotation, for instance, has been identified as a significant risk factor for dislocation following reconstruction procedures, as it alters joint biomechanics and load distribution (34–36)

According to the International Society of Biomechanics, the hip joint is considered a ball-and-socket joint and its center of rotation is defined at the center of the hip joint, even if incongruities exist (37). Radiographically, it can be estimated by fitting a circle to the contour of the femoral head on anteroposterior pelvic X-rays. On computed tomography (CT), a three-dimensional (3D) reconstruction enables determination of the center of rotation by placing a virtual sphere over the femoral head.

Acetabular orientation is described using anteversion and inclination. In this thesis, radiographic definitions according to Murray are used (38). Radiographic inclination is defined as the angle between the acetabular axis and the longitudinal axis projected onto the coronal plane. Radiographic anteversion is defined as the angle between the acetabular axis and the coronal plane (Figure 1.4). Anteversion and inclination can also be measured on CT. Although the coronal plane itself is not directly measurable in CT-based pelvic models, it can be approximated using the anterior pelvic plane (APP), often defined by the anterior superior iliac spines (ASIS) and the pubic tubercles (39). The APP has been shown to be almost parallel to the true coronal plane when the patient is in a supine or erect position (40).

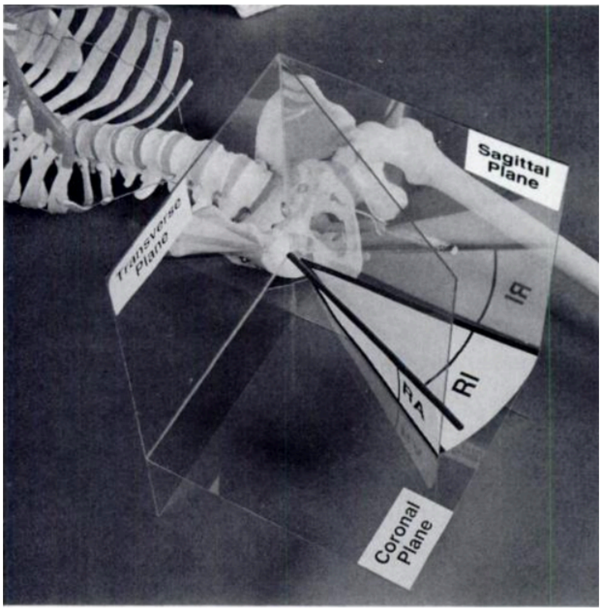

Figure 1.4. Visual representation of radiographic inclination and radiographic anteversion as outlined by Murray (38).

1.7 Outline of this thesis

These biomechanical considerations emphasize the importance of accurate restoration of the hip center and precise orientation of the acetabular component to achieve optimal postoperative outcomes and minimize complications. In this thesis, both preoperative measurements (native hip anatomy) and postoperative measurements (after implantation) are considered. CT imaging is generally regarded as the most precise technique for such measurements, whereas plain radiography (X-ray) is more widely available and cost-effective. However, it remains unclear whether X-ray allows equally reliable measurements in the context of LUMiC reconstructions. First, existing literature is reviewed providing an overview of existing measurement methods for assessing hip and implant positioning, focusing mainly on studies involving conventional total hip arthroplasties. This is followed by an analysis of LUMiC cases, beginning with a subanalysis comparing X-ray and CT-based measurements in LUMC patients to assess the accuracy of radiographs for determining LUMiC component position. The main study consists of a multicenter, CT-based evaluation of LUMiC prosthesis positioning and its association with dislocation risk. Supplementary materials include detailed measurement protocols, illustrative cases and calculations.

References

1. Chaudhry SR, Nahian A, Chaudhry K. Anatomy, Abdomen and Pelvis, Pelvis. In: StatPearls. StatPearls Publishing; 2023.
2. DeSilva JM, Rosenberg KR. Anatomy, Development, and Function of the Human Pelvis. Anatomical record (Hoboken, NJ : 2007). 2017 Apr;300(4).
3. ditki medical & biological sciences [Internet]. [cited 2025 Aug 6]. Gross Anatomy Glossary: Pelvic Girdle. Available from: http://ditki.com/course/gross-anatomy/glossary/gross-anatomic-microscopic-structure/pelvic-girdle
4. Gatta G, Capocaccia R, Botta L, Mallone S, De Angelis R, Ardanaz E, et al. Burden and centralised treatment in Europe of rare tumours: results of RARECAREnet-a population-based study. The Lancet Oncology. 2017 Aug;18(8).
5. Epidemiology of bone and soft-tissue sarcomas. Orthopaedics and Trauma. 2017 Jun 1;31(3):144–50.
6. de Pinieux G, Karanian M, Le Loarer F, Le Guellec S, Chabaud S, Terrier P, et al. Nationwide incidence of sarcomas and connective tissue tumors of intermediate malignancy over four years using an expert pathology review network. PloS one. 2021 Feb 25;16(2).
7. Galasko CS. Skeletal metastases. Clinical orthopaedics and related research. 1986 Sep;(210).
8. Coleman RE. Clinical features of metastatic bone disease and risk of skeletal morbidity. Clinical cancer research : an official journal of the American Association for Cancer Research. 2006 Oct 15;12(20 Pt 2).
9. Coleman R, Hadji P, Body JJ, Santini D, Chow E, Terpos E, et al. Bone health in cancer: ESMO Clinical Practice Guidelines. Annals of oncology : official journal of the European Society for Medical Oncology. 2020 Dec;31(12).
10. Guzik G. Treatment of metastatic lesions localized in the acetabulum. Journal of orthopaedic surgery and research. 2016 Apr 28;11(1).
11. Strauss SJ, Frezza AM, Abecassis N, Bajpai J, Bauer S, Biagini R, et al. Bone sarcomas: ESMO-EURACAN-GENTURIS-ERN PaedCan Clinical Practice Guideline for diagnosis, treatment and follow-up. Annals of oncology : official journal of the European Society for Medical Oncology. 2021 Dec;32(12).
12. Capanna R, van Horn JR, Guernelli N, Briccoli A, Ruggieri P, Biagini R, et al. Complications of pelvic resections. Archives of orthopaedic and traumatic surgery Archiv fur orthopadische und Unfall-Chirurgie. 1987;106(2).
13. Fisher NE, Patton JT, Grimer RJ, Porter D, Jeys L, Tillman RM, et al. Ice-cream cone reconstruction of the pelvis: a new type of pelvic replacement: early results. The Journal of bone and joint surgery British volume. 2011 May;93(5).
14. Grimer RJ, Chandrasekar CR, Carter SR, Abudu A, Tillman RM, Jeys L. Hindquarter amputation: is it still needed and what are the outcomes? The bone & joint journal. 2013 Jan;95-B(1).
15. Enneking WF, Dunham WK. Resection and reconstruction for primary neoplasms involving the innominate bone. The Journal of bone and joint surgery American volume. 1978 Sep;60(6).
16. Bus MP, Boerhout EJ, Bramer JA, Dijkstra PD. Clinical outcome of pedestal cup endoprosthetic reconstruction after resection of a peri-acetabular tumour. The bone & joint journal. 2014 Dec;96-B(12).
17. Lenze U, Kasal S, Hefti F, Krieg AH. Non-vascularised fibula grafts for reconstruction of segmental and hemicortical bone defects following meta- /diaphyseal tumour resection at the extremities. BMC musculoskeletal disorders. 2017 Jul 5;18(1).
18. Xu S, Guo Z, Shen Q, Peng Y, Li J, Li S, et al. Reconstruction of Tumor-Induced Pelvic Defects With Customized,

Three-Dimensional Printed Prostheses. Frontiers in oncology. 2022 Jun 30;12.

19. Brown TS, Salib CG, Rose PS, Sim FH, Lewallen DG, Abdel MP. Reconstruction of the hip after resection of periacetabular oncological lesions: a systematic review. The bone & joint journal. 2018 Jan;100-B(1 Supple A).

20. Fujiwara T, Ogura K, Christ A, Bartelstein M, Kenan S, Fabbri N, et al. Periacetabular reconstruction following limb-salvage surgery for pelvic sarcomas. Journal of bone oncology. 2021 Oct 18;31.

21. Bus MPA, Szafranski A, Sellevold S, Goryn T, Jutte PC, Bramer JAM, et al. LUMiC® Endoprosthetic Reconstruction After Periacetabular Tumor Resection: Short-term Results. Clinical Orthopaedics and Related Research. 2016 Mar 28;475(3):686.

22. MUTARS® LUMiC® [Internet]. [cited 2025 Aug 6]. Available from: https://www.implantcast.de/en/for-medical-professionals/products/standard-/-tumour-prosthetics/pelvis-and-hip-endoprosthetics/revision-and-tumour-endoprosthetics/mutarsr-lumicr/

23. Bus MPA, Campanacci DA, Albergo JI, Leithner A, van de Sande MAJ, Gaston CL, et al. Conventional Primary Central Chondrosarcoma of the Pelvis: Prognostic Factors and Outcome of Surgical Treatment in 162 Patients. JBJS. 2018 Feb 21;100(4):316.

24. Henderson ER, O'Connor MI, Ruggieri P, Windhager R, Funovics PT, Gibbons CL, et al. Classification of failure of limb salvage after reconstructive surgery for bone tumours : a modified system Including biological and expandable reconstructions. The bone & joint journal. 2014 Nov;96-B(11).

25. Rizkallah M, Ferguson PC, Basile G, Kim P, Werier J, Wilson D, et al. LUMiC® endoprosthesis for pelvic reconstruction: A Canadian experience. Journal of surgical oncology. 2023 Mar;127(4).

26. Evenhuis RE, van de Sande MAJ, Fiocco M, Dierselhuis EF, Broekhuis D, Bus MPA. LUMiC Endoprosthetic Reconstruction of Periacetabular Tumor Defects: A Multicenter Follow-up Study. The Journal of bone and joint surgery American volume. 2024 Jul 17;106(14).

27. Baghdadi YM, Larson AN, Sierra RJ. Restoration of the hip center during THA performed for protrusio acetabuli is associated with better implant survival. Clinical orthopaedics and related research. 2013 Oct;471(10).

28. García-Rey E, García-Cimbrelo E. Abductor Biomechanics Clinically Impact the Total Hip Arthroplasty Dislocation Rate: A Prospective Long-Term Study. The Journal of arthroplasty. 2016 Feb;31(2).

29. Kummer FJ, Shah S, Iyer S, DiCesare PE. The effect of acetabular cup orientations on limiting hip rotation. The Journal of arthroplasty. 1999 Jun;14(4).

30. D'Lima DD, Urquhart AG, Buehler KO, Walker RH, Colwell CW. The effect of the orientation of the acetabular and femoral components on the range of motion of the hip at different head-neck ratios. The Journal of bone and joint surgery American volume. 2000 Mar;82(3).

31. Murphy WS, Yun HH, Hayden B, Kowal JH, Murphy SB. The Safe Zone Range for Cup Anteversion Is Narrower Than for Inclination in THA. Clinical orthopaedics and related research. 2018 Feb;476(2).

32. Wan Z, Boutary M, Dorr LD. The influence of acetabular component position on wear in total hip arthroplasty. The Journal of arthroplasty. 2008 Jan;23(1).

33. Delp SL, Maloney W. Effects of hip center location on the moment-generating capacity of the muscles. Journal of biomechanics. 1993 Apr;26(4-5).

34. Qu H, Mou H, Wang K, Tao H, Huang X, Yan X, et al. Risk factor investigation for hip dislocation after periacetabular tumour resection and endoprosthetic reconstruction via thin-slice CT-based 3D model. Bone Joint J. 2022 Oct;104-B(10):1180–8.

35. Wang H, Tang X, Ji T, Yan T, Yang R, Guo W. Risk factors for early dislocation of the hip after periacetabular tumour resection and endoprosthetic reconstruction of the hemipelvis. Bone Joint J. 2021 Feb;103-B(2):382–90.

36. Sariali E, Klouche S, Mamoudy P. Investigation into three dimensional hip anatomy in anterior dislocation after THA. Influence of the position of the hip rotation centre. Clin Biomech (Bristol). 2012 Jul;27(6):562–7.

37. Wu G, Siegler S, Allard P, Kirtley C, Leardini A, Rosenbaum D, et al. ISB recommendation on definitions of joint coordinate system of various joints for the reporting of human joint motion--part I: ankle, hip, and spine. International Society of Biomechanics. Journal of biomechanics. 2002 Apr;35(4).

38. Murray DW. The definition and measurement of acetabular orientation. The Journal of bone and joint surgery British volume. 1993 Mar;75(2).

39. Wang RY, Xu WH, Kong XC, Yang L, Yang SH. Measurement of acetabular inclination and anteversion via CT generated 3D pelvic model. BMC Musculoskeletal Disorders. 2017 Aug 29;18(1):1–7.

40. Stylianides GA, Beaulieu M, Dalleau G, Rivard CH, Allard P. Iliac crest orientation and geometry in able-bodied and non-treated adolescent idiopathic scoliosis girls with moderate and severe spinal deformity. European spine journal : official publication of the European Spine Society, the European Spinal Deformity Society, and the European Section of the Cervical Spine Research Society. 2012 Apr;21(4).

2

Introduction

Surgical treatment of pelvic bone tumors remains a significant challenge in the field of orthopedic oncology (1). Pelvic tumors are often diagnosed late due to their potential to attain substantial sizes before detection. As a result, resection presents unique challenges, including the risk of inadequate surgical margins and increased susceptibility to infection, especially in lengthy procedures (2). Achieving a successful reconstruction following resection is further complicated, given the extensive bone and soft tissue removal and the resultant biomechanical stresses on reconstructions.

Traditionally, hindquarter amputation was the predominant treatment option, although it was often associated with poor cosmetic, functional and psychological outcomes (3,4). Fortunately, advances in imaging, adjuvant therapies, surgical techniques and implant design have expanded eligibility for limb-salvaging surgery, such as internal hemipelvectomy (5,6). However, many of the implants developed for this purpose have been associated with a disappointing frequency of both mechanical and non-mechanical complications and failures (7–9), as categorized by Henderson et al (10).

In light of these challenges, the development of a novel implant design aims to address shortcomings observed with previous prosthetic solutions. The LUMiC prosthesis (Implantcast, Buxtehude, Germany) has been employed since 2008 (11). It is designed to facilitate easy and durable fixation, even in cases with limited remaining bone. Nevertheless, as with all periacetabular reconstruction techniques, the risk of complications remains substantial. Dislocation rates of 13% and 19% have been reported by Bus et al. (2017) and Evenhuis et al. (2024), respectively (11,12). Existing literature on other prostheses highlights the importance of factors such as an altered position of the center of rotation (COR) in contributing to postoperative complications, particularly dislocation (13–15). However, the specific impact of COR on dislocation risk in patients reconstructed with the LUMiC prosthesis remains unclear.

Building upon a previously developed semi-automatic method for comparing preoperative planning with the postoperative position of prosthetic components, this study applies a similar approach to assess the positioning of the LUMiC prosthesis (16,17). This method allows for a standardized evaluation of deviations in COR, anteversion (AV) and inclination (INCL) based on preoperative and postoperative computed tomography (CT) data. The aim of this study was to determine whether such deviations are associated with the occurrence of dislocation.

3

Methods

3.1 Study design

An international multicenter retrospective cohort study was conducted on patients who underwent internal hemipelvectomy for a bone tumor and received a LUMiC prosthesis between 2008 and 2022. The primary outcome measures were dislocation rate and its association with changes in the COR, AV and INCL. Approval for conducting the study was obtained from the ethical committee of the Leiden University Medical Center (LUMC). The committee determined that patient informed consent was not applicable (W.24.013/2024-058). Participating centers received approval from their local ethical review boards.

3.2 Patient selection

Centers from the previous multicenter LUMiC study by Evenhuis et al. (12) were recruited to participate in the present study. Participating centers were asked to upload preoperative and postoperative pelvic CT scans for eligible patients; relevant clinical data had already been collected in the earlier study.

Patients were eligible for inclusion if they met the following criteria:

- Age ≥16 years
- Treated with an internal hemipelvectomy for a pelvic bone tumor
- Reconstruct with a LUMiC prosthesis
- Availability of at least one postoperative (PET-)CT scan of the pelvis with a slice thickness ≤3 mm
- Minimum follow-up of 12 months post-surgery

Preferably, a preoperative CT scan was available. In cases where no preoperative scan was present, the contralateral (healthy) side from the postoperative CT was used for comparison.

Patients were excluded if:

- The internal hemipelvectomy involved resection of the medial ilium (Modified Enneking zone 1A (8,18)), resulting in LUMiC fixation into the sacrum
- CT imaging data was unavailable or of insufficient quality for accurate anatomical assessment

Patients from participating centers without suitable CT scans were still included in analyses comparing the characteristics between patients with and without CT data, as well as in calculating the cumulative incidence of dislocation.

3.3 Positioning analysis

For each patient, pre- and postoperative pelvic CT scans closest to the date of surgery were used for analysis. Employing semi-automatic image analysis and modeling software (Mimics 26; Materialise, Leuven, Belgium), three-dimensional (3D) surface models were generated from the pre- and postoperative CT scans. Thereafter, the postoperative pelvic model was aligned with the preoperative pelvic model using surface-based matching techniques (3-Matic 18.0; Materialise, Leuven, Belgium). Matching was performed on the contralateral hemipelvis (the side unaffected by the pelvic tumor) with the sacrum excluded.

In cases where a preoperative CT scan was not available, the contralateral (healthy) hemipelvis of the postoperative model was mirrored and aligned onto the affected side using surface matching. This approach was used to approximate the preoperative anatomy, assuming bilateral symmetry of the pelvis (19).

Next, anatomical landmarks were identified in the preoperative 3D model to define the pelvic reference planes. The anterior pelvic plane (APP) was determined based on the method described by Wang et al. to approximate the coronal plane of the pelvis. The APP was delineated by a plane passing through the left anterior superior iliac spine (ASIS), right ASIS and the midpoint of the pubic tubercles (PT) (20). The sagittal plane was then defined by two points on the sacral crest (SC) and constrained to be perpendicular to the coronal plane. Finally, the transversal plane was computed as a plane perpendicular to both the coronal and sagittal planes, passing through the left ASIS point. See Figure 1.1 for a representation of the landmark positions.

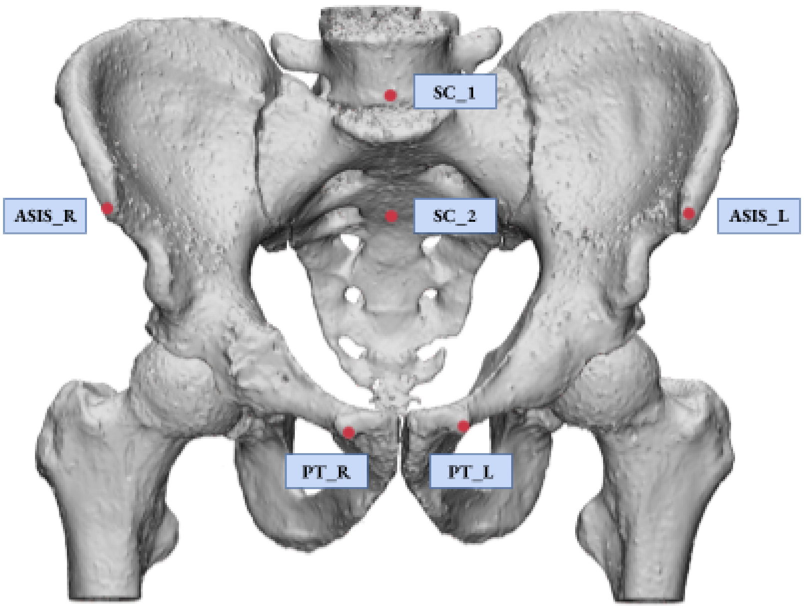

Figure 3.1. Representation of the anatomical landmark positions. Points on the left and right anterior superior iliac spine (ASIS_L and ASIS_R). Two points on the sacral crest (SC_1 and SC_2). Points on the left and right pubic tubercle (PT_L and PT_R).

To quantify the AV and INCL angles, a plane through the acetabular rim was defined. Nine landmarks were equally positioned on the preoperative model (Figure 3.2) and the acetabular plane was computed using the mean squared difference method, based on Wang et al. (20). For the postoperative acetabular plane only three landmarks were positioned (Figure 3.3), considering the flat surface of the prosthesis. The AV and INCL angles were calculated according to the radiographic definitions described by Murray (21). Radiographic AV is defined as the angle between the acetabular axis and the coronal plane. Radiographic INCL is defined as the angle between the acetabular axis and the longitudinal axis projected onto the coronal plane.

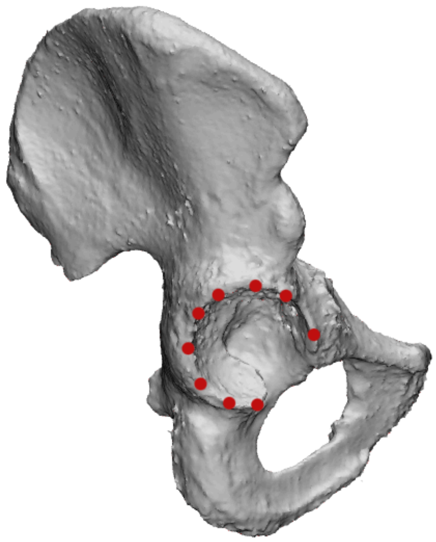

Figure 3.2. Representation of the nine landmarks placed on the acetabular rim of the preoperative model.

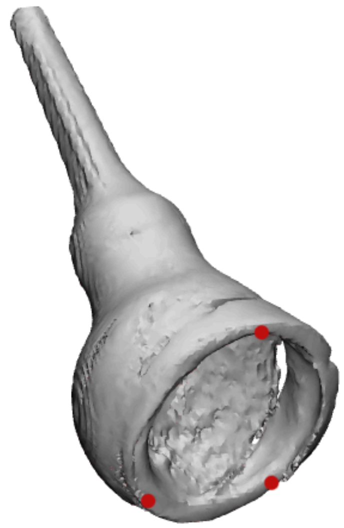

Figure 3.3. Representation of the three landmarks placed on the LUMiC in the postoperative model.

COR was defined by fitting a sphere on the femoral and prosthesis head for the pre- and postoperative models as illustrated in Figure 3.4 and 3.5, respectively. Displacement of the COR was calculated using a transformation matrix to describe displacement in mediolateral (ML), anteroposterior (AP) and superoinferior (SI) direction, with positive values for medial, posterior and superior translation. The vector length was calculated to determine the total displacement of the COR.

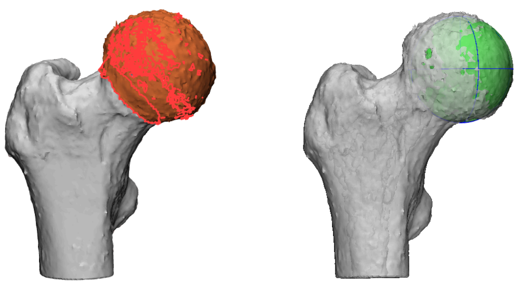

Figure 3.4. Determining preoperative center of rotation. Marking the femoral head (left) and surface matching of a sphere (right).

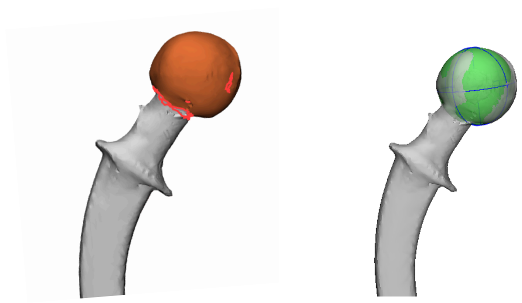

Figure 3.5. Determining postoperative center of rotation. Marking the prosthesis head (left) and surface matching of a sphere (right).

The coordinates of all points and the centers of the spheres were exported to determine the deviations in pre- and postoperative situations. All calculations were executed using a Python script (Python 3.11; Python Software Foundation). The coordinates of all landmarks and midpoints of the rotation centers were imported for analysis. See Appendix A for the full measurement protocol and Appendix B for the Python calculations.

3.4 Statistics

Patient demographics were summarized using the mean and standard deviation (SD) or the median and interquartal range (IQR) for continuous variables (depending on data distribution) and as frequency and percentage for categorical variables. Comparisons between the measured CT group and the non-measured group were conducted to assess whether the measured CT group was representative of the overall cohort. Unpaired t-tests were used for normally distributed continuous variables and while Mann–Whitney U tests were applied for non-normally distributed variables. Categorical variables were compared using the chi-squared test or Fisher's exact test.

Differences between pre- and postoperative LUMiC positioning parameters, including AV, INCL and COR, were quantified using both signed and unsigned measures. Signed mean ± SD were reported to indicate the direction of change, whereas unsigned mean ± SD were used to represent total absolute differences.

Cox proportional hazards regression models were used to assess associations between LUMiC positioning and postoperative dislocation risk. Separate univariate models were constructed for COR (total, ML, AP and SI), AV (postoperative and difference) and INCL (postoperative and difference). Hazard ratios (HRs) with 95% confidence intervals (CIs) were reported. To estimate the cumulative incidence of dislocation, competing risks models were used accounting for death as competing event (22). Data analyses were conducted using SPSS version 29.0 (IBM) and RStudio version 4.5.1 (23). Statistical significance was set at $p < 0.05$.

4

Results

4.1 Patient characteristics

Of the 14 centers that participated in the previous LUMiC study, 9 centers contributed to the current analysis, comprising 114 of 166 eligible patients. Of these, 69 patients had at least one postoperative CT scan available, of which 60 were of sufficient quality for measurement. Nine scans were excluded due to slice thickness > 3 mm, severe pelvic dissociation or prior contralateral surgery preventing reconstruction of the preoperative anatomy.

The measured CT cohort thus consisted of 60 patients, including 42 with a preoperative CT scan. For the remaining 18 patients, the contralateral (unaffected) side from the postoperative scan was mirrored to approximate preoperative anatomy. The median interval from surgery to postoperative CT was 53 days (IQR 3–201).

In the measured CT group, the mean age at surgery was 53.0 ± 16.6 years and 48% of patients were male. The mean body mass index (BMI) was 25.6 ± 4.0 kg/m^2. The majority of patients were classified as American Society of Anesthesiologists (ASA) 2 (65%). The mean surgical time was 5.9 ± 2.2 hours and the mean blood loss was 2002 ± 1461 mL. The most common resection type was P2 (50%), followed by P2+3 (35%) and P1b+2 (7%). A cemented LUMiC stem was used in 13% of cases, a dual mobility cup in 68% and a silver-coated cup in 32%. Dislocation (Henderson 1A) occurred in 11 (18%) patients.

Characteristics were largely comparable between the measured CT group and the remaining patient population, with the exception of ASA classification, which differed significantly: the measured group included a higher proportion of ASA I and II patients ($p = 0.023$). A detailed summary of patient characteristics, surgical details and dislocation rates is presented in Table 4.1.

Table 4.1. Patient characteristics, surgical details and dislocation rates. Comparison between patients with and without CT-based measurements

Characteristic	Not measured (n = 54)	CT measured group (n = 60)	p-value
Age at surgery (mean ± SD)	53.1 ± 18.3	53.0 ± 16.6	0.965
Sex, male	28 (51.9)	29 (48.3)	0.708
Mean BMI (mean kg/m² ± SD)	25.5 ± 3.8	25.6 ± 4.0	0.876
ASA score	53	60	0.023
ASA1	5 (9.4)	12 (20.0)	
ASA2	29 (54.7)	39 (65.0)	
ASA3	19 (35.8)	9 (15.0)	
Smoking	44	46	0.448
No	34 (77.3)	33 (71.7)	
Yes, currently	6 (13.6)	7 (15.2)	
Yes, formerly	4 (9.1)	6 (13.0)	
Diagnosis	54	60	0.844
Osteosarcoma	5 (9.3)	6 (10.0)	
Chondrosarcoma	22 (40.7)	22 (36.7)	
Ewing sarcoma	4 (7.4)	2 (3.3)	
Soft tissue sarcoma	1 (1.9)	1 (1..7)	
Metastasis	16 (29.6)	18 (30.0)	
Other	6 (11.1)	11 (18.3)	
Previous surgery at same side	17 (31.5)	10 (16.7)	0.079*
Time surgery in hours (mean ± SD)	5.4 ± 1.9	5.9 ± 2.2	0.210
Blood loss in mL (mean ± SD)	1702 ± 1307	2002 ± 1461	0.317
Modified Enneking resection type			0.984
P1b+2	4 (7.4)	4 (6.7)	
P2	29 (53.7)	30 (50.0)	
P2+3	16 (29.6)	21 (35.0)	
P1b+2+3	2 (3.7)	2 (3.3)	
Other	3 (5.6)	3 (5.0)	
Cemented LUMiC stem	15 (27.8)	8 (13.3)	0.065*
Cup size			0.427
50 mm	11 (20.8)	14 (23.7)	
54 mm	22 (41.5)	21 (35.6)	
60 mm	20 (37.7)	24 (40.7)	
Silver-coated cup	9 (16.7)	19 (31.7)	0.082*
Dual mobility cup	38/54 (70.4)	40/59 (67.8)	0.768
Dislocation	14 (25.9)	11 (18.3)	0.952

*Values are presented as numbers, with percentages in parentheses, unless otherwise specified. ASA = American Society of Anesthesiologists physical status, BMI = body mass index. *=p-value calculated using Fisher's exact test.*

4.2 Comparison AV, INCL and COR

The signed mean change in AV was 9.0 ± 13.7° and in INCL -14.1 ± 15.6°. COR shifted on average 4.7 ± 13.7 mm laterally (ML), 0.7 ± 14.7 mm anteriorly (AP) and 16.0 ± 16.2 mm superiorly (SI), resulting in a total displacement of 27.1 ± 14.2 mm.

The mean unsigned differences were 13.3° ± 9.4 for AV and 16.9° ± 12.6 for INCL. Unsigned COR displacements measured 10.5 ± 9.9 mm (ML), 11.4 ± 9.1 mm (AP) and 18.2 ± 13.6 mm (SI) (Table 4.2).

Table 4.2. Comparison of pre- and postoperative cup positioning parameters

	AV (°)			INCL (°)			Displacement COR (mm)			
	pre	post	Δ	pre	post	Δ	ML	AP	SI	total
signed mean	16.3	25.3	9.0	51.7	37.6	-14.1	-4.7	-0.7	16.0	27.1
SD	6.1	14.3	13.7	4.8	16.1	15.6	13.7	14.7	16.2	14.2
unsigned mean			13.3			16.9	10.5	11.4	18.2	
SD			9.4			12.5	9.9	9.1	13.6	

Anteversion (AV), inclination (INCL) and displacement of the center of rotation (COR) before and after surgery. Values are presented as mean including standard deviation (SD). Positive values indicate medial, posterior and superior translation of the COR.
Δ = difference (post - pre); ML=mediolateral; AP=anteroposterior; SI=superoinferior.

4.3 Risk factors for dislocation

In univariate (crude) Cox regression analyses, medialization of the COR was significantly associated with an increased risk of dislocation (HR = 1.070, 95% CI: 1.012–1.132, p = 0.018). No significant associations were observed for the other components of the COR, including COR total (p = 0.829), COR AP (p = 0.381) and COR SI (p = 0.205). Neither postoperative AV nor INCL, nor their differences from preoperative values, were significantly associated with dislocation risk (Table 4.3).

Table 4.3. Univariate Cox proportional hazards models for risk of postoperative dislocation (n = 60, 11 events)

Variable	HR_{CR}	95% CI	p-value
COR total (mm)	1.005	0.964 - 1.047	0.829
COR ML (mm)	1.070	1.012 - 1.132	0.018
COR AP (mm)	1.018	0.978 - 1.059	0.381
COR SI (mm)	1.023	0.987 - 1.061	0.205
AV postoperative (°)	1.028	0.987 - 1.070	0.183
AV difference (°)	1.031	0.986 - 1.078	0.182
INCL postoperative (°)	1.006	0.967 - 1.047	0.757
INCL difference (°)	1.009	0.970 - 1.050	0.650

COR=center of rotation; ML=mediolateral; AP=anteroposterior; SI=superoinferior; AV=anteversion; INCL= inclination; HR_{CR}= crude hazard ratio; CI=confidence interval.

4.4 Cumulative incidence of dislocation

The cumulative incidence of dislocation was estimated using a competing risks model accounting for death as a competing event. Over the follow-up period, 25 dislocations occurred among 114 patients. The cumulative incidence over time is shown in Figure 4.1.

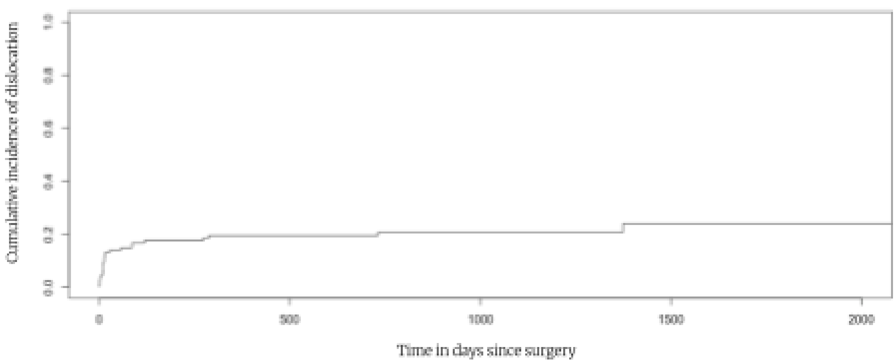

Figure 4.1. Cumulative incidence of dislocation, using a competing risks model.

5

Discussion

This study represents the first quantitative analysis of the LUMiC prosthesis position in terms of AV, INCL and COR displacement using postoperative CT imaging and its association with dislocation risk. These findings provide novel insights into how specific positional changes relate to clinical outcomes following reconstruction with this implant.

The primary positional changes observed were a mean increase in AV by 9.0°, a mean decrease in INCL by 14.2° and substantial COR displacement, predominantly in the superior (16.0 mm) and lateral (4.7 mm) directions. The mean total COR displacement was 27.1 mm. These results are consistent with findings reported in literature (24). Previous studies have reported that superolateral relocation of the COR causes significant increases in total hip joint force due to a reduced moment arm of the hip adductors, which affects joint biomechanics (25–27).

In this analysis, medialization of the COR was significantly associated with an increased risk of postoperative dislocation (HR 1.07 per millimeter medial shift, $p = 0.018$). This finding aligns with biomechanical principles and previous literature, suggesting that medialization may reduce soft-tissue tension and fail to adequately restore femoral offset, both essential for maintaining joint stability (14,15). In contrast, lateralization of the COR likely preserves native biomechanics and soft-tissue tension, contributing to improved implant stability and a lower risk of dislocation. Neither postoperative AV nor INCL, nor their changes from preoperative values, showed significant associations with dislocation risk in this cohort, which contrasts with findings reported in literature (28,29).

Beyond implant positioning, previous studies have shown that resection extent and prior surgery are also associated with dislocation risk (11,12). These factors may affect both soft-tissue integrity and biomechanical stability. In future, larger studies should include multivariate analyses to identify which variables contribute most to postoperative instability.

Strengths of the present study include the use of a standardized, reproducible CT-based method to quantify three-dimensional positional changes. The relatively large, multicenter cohort is notable given the rarity of this patient group. Additionally, the use of mirrored contralateral anatomy to approximate preoperative positioning helped to overcome the lack of preoperative scans in some cases enabling inclusion of a larger patient group.

However, several limitations should be considered. The modest sample size, combined with the limited number of dislocation events, restricted the study's statistical power. Postoperative CT scans were acquired at varying time points (IQR 3–201 days), which may have allowed for implant migration in some cases, introducing measurement heterogeneity. Postoperative CT scans were not available for all patients, which may introduce selection bias. In addition, the study population was heterogeneous, with various indications for LUMiC implantation and large differences in resection extent. These factors may affect soft-tissue tension and joint stability, adding further variability to the risk of dislocation and potentially confounding the association with implant position.

Furthermore, preoperative CT scans were missing in some cases; although mirroring of the contralateral pelvis was used to approximate preoperative anatomy, this approach is challenging when large postoperative defects are present, resulting in reduced bone surface area for accurate fitting of the mirrored pelvis and potentially decreasing measurement precision. In this study, matching was performed using only the hemipelvis, without including the sacrum. This approach may be suboptimal, especially in cases with sacroiliac joint deformation, where alternative matching strategies, such as including the sacrum or the entire intact pelvis, could potentially improve alignment accuracy. It was not investigated which matching method is most accurate, representing an area for future validation. Finally, no inter- or intraobserver reliability testing was performed, which limits insight into the reproducibility of our measurements.

Future research should focus on larger, prospectively collected cohorts with standardized postoperative imaging intervals, to allow robust multivariable analysis of risk factors. These should incorporate implant position, resection extent, prior surgeries and other patient- or surgery-specific variables that may affect soft-tissue tension and stability. Longitudinal imaging studies could assess temporal stability of implant positioning and provide insight into potential migration. To address measurement reproducibility, further validation of the current methodology through inter- and intraobserver consistency studies is recommended.

6

Conclusion

In conclusion, this study demonstrates that medial displacement of the COR after LUMiC prosthesis implantation may contribute to an increased risk of dislocation, whereas SI and AP displacement of the COR, as well as INCL and AV, were not associated with dislocation in the current analysis. These findings suggest the potential importance of restoring native hip biomechanics in pelvic reconstruction and may inform considerations for implant positioning strategies to improve postoperative stability.

Acknowledgements

Members of the LUMiC® study group include Prof. Paul Jutte, Edwin Dierselhuis, MD, PhD, Daniel Rau, MD, PhD, Maurizio Scorianz, MD, PhD, Thomas Hilton, MD, Schalk Klopper, MD, Prof. Thomas Schubert, MD, PhD, Sebastian G. Walter, MD, MD, Marko Bergovec, MD, PhD, Silvan Wittenberg, MD

References

1. Fujiwara T, Ogura K, Christ A, Bartelstein M, Kenan S, Fabbri N, et al. Periacetabular reconstruction following limb-salvage surgery for pelvic sarcomas. Journal of Bone Oncology. 2021 Dec;31.

2. Angelini A, Drago G, Trovarelli G, Calabrò T, Ruggieri P. Infection after surgical resection for pelvic bone tumors: an analysis of 270 patients from one institution. Clin Orthop Relat Res. 2014 Jan;472(1).

3. Daigeler A, Lehnhardt M, Khadra A, Hauser J, Steinstraesser L, Langer S, et al. Proximal major limb amputations--a retrospective analysis of 45 oncological cases. World J Surg Oncol. 2009 Feb 9;7.

4. Grimer RJ, Chandrasekar CR, Carter SR, Abudu A, Tillman RM, Jeys L. Hindquarter amputation: is it still needed and what are the outcomes? Bone Joint J. 2013 Jan;95-B(1).

5. Fisher NE, Patton JT, Grimer RJ, Porter D, Jeys L, Tillman RM, et al. Ice-cream cone reconstruction of the pelvis: a new type of pelvic replacement: early results. J Bone Joint Surg Br. 2011 May;93(5).

6. Puri A, Pruthi M, Gulia A. Outcomes after limb sparing resection in primary malignant pelvic tumors. Eur J Surg Oncol. 2014 Jan;40(1).

7. Jansen JA, van de Sande MA, Dijkstra PD. Poor long-term clinical results of saddle prosthesis after resection of periacetabular tumors. Clin Orthop Relat Res. 2013 Jan;471(1).

8. Bus MP, Boerhout EJ, Bramer JA, Dijkstra PD. Clinical outcome of pedestal cup endoprosthetic reconstruction after resection of a peri-acetabular tumour. Bone Joint J. 2014 Dec;96-B(12).

9. Ozaki T, Hoffmann C, Hillmann A, Gosheger G, Lindner N, Winkelmann W. Implantation of hemipelvic prosthesis after resection of sarcoma. Clin Orthop Relat Res. 2002 Mar;(396).

10. Henderson ER, O'Connor MI, Ruggieri P, Windhager R, Funovics PT, Gibbons CL, et al. Classification of failure of limb salvage after reconstructive surgery for bone tumours : a modified system Including biological and expandable reconstructions. Bone Joint J. 2014 Nov;96-B(11).

11. Bus MPA, Szafranski A, Sellevold S, Goryn T, Jutte PC, Bramer JAM, et al. LUMiC Endoprosthetic Reconstruction After Periacetabular Tumor Resection: Short-term Results. Clin Orthop Relat Res. 2017 Mar;475(3):686–95.

12. Evenhuis RE, van de Sande MAJ, Fiocco M, Dierselhuis EF, Broekhuis D, Bus MPA, et al. LUMiC Endoprosthetic Reconstruction of Periacetabular Tumor Defects: A Multicenter Follow-up Study. J Bone Joint Surg Am. 2024 Jul 17;106(14):1309–16.

13. Qu H, Mou H, Wang K, Tao H, Huang X, Yan X, et al. Risk factor investigation for hip dislocation after periacetabular tumour resection and endoprosthetic reconstruction via thin-slice CT-based 3D model. Bone Joint J. 2022 Oct;104-B(10).

14. Wang H, Tang X, Ji T, Yan T, Yang R, Guo W. Risk factors for early dislocation of the hip after periacetabular tumour resection and endoprosthetic reconstruction of the hemipelvis. Bone Joint J. 2021 Feb;103-B(2).

15. Sariali E, Klouche S, Mamoudy P. Investigation into three dimensional hip anatomy in anterior dislocation after THA. Influence of the position of the hip rotation centre. Clinical biomechanics (Bristol, Avon). 2012 Jul;27(6).

16. Meurs W. Accuracy of Positioning Custom Triflange Acetabular Components in THA Revision and Tumor Resection Surgery – A 3D-CT Assessment Stud. 2021 [cited 2024 Feb 29]; Available from: https://repository.tudelft.nl/islandora/object/uuid%3A551ee277-3e7a-4219-86df-cc906e48bd24

17. Broekhuis D, Meurs WMH, Kaptein BL, Karunaratne S, Rl CS, Sommerville S, et al. High accuracy of positioning custom triflange acetabular components in tumour and total hip arthroplasty revision surgery. Bone & joint open. 2024 Apr 1;5(4).

18. Enneking WF, Dunham WK. Resection and reconstruction for primary neoplasms involving the innominate bone. J Bone Joint Surg Am. 1978 Sep;60(6).

19. Kim SC, Lim YW, Kwon SY, Lee JK, Park IK, Kim YS. Comparative Analysis of Radiographic Hip Joint Geometry Using Measurement Tools on Picture Archiving and Communication System: A Prospective Study of 100 Pelvic Radiographs of Koreans. J Arthroplasty. 2016 Nov;31(11):2597–602.

20. Wang RY, Xu WH, Kong XC, Yang L, Yang SH. Measurement of acetabular inclination and anteversion via CT generated 3D pelvic model. BMC Musculoskelet Disord. 2017 Aug 29;18(1):1–7.

21. Murray DW. The definition and measurement of acetabular orientation. J Bone Joint Surg Br. 1993 Mar;75(2):228–32.

22. Putter H, Fiocco M, Geskus RB. Tutorial in biostatistics: competing risks and multi-state models. Stat Med. 2007 May 20;26(11):2389–430.

23. The R Project for Statistical Computing [Internet]. [cited 2025 Jun 2]. Available from: https://www.r-project.org/

24. Kim SC, Lim YW, Kwon SY, Jo WL, Ju SH, Park CJ, et al. Level of surgical experience is associated with change in hip center of rotation following cementless total hip arthroplasty: A radiographic assessment. PloS one. 2017 May 24;12(5).

25. Delp SL, Wixson RL, Komattu AV, Kocmond JH. How superior placement of the joint center in hip arthroplasty affects the abductor muscles. Clinical orthopaedics and related research. 1996 Jul;(328).

26. Doehring TC, Rubash HE, Shelley FJ, Schwendeman LJ, Donaldson TK, Navalgund YA. Effect of superior and superolateral relocations of the hip center on hip joint forces. An experimental and analytical analysis. The Journal of arthroplasty. 1996 Sep;11(6).

27. Iglic A, Antolic V, Srakar F. Biomechanical analysis of various operative hip joint rotation center shifts. Archives of orthopaedic and trauma surgery. 1993;112(3).

28. Biedermann R, Tonin A, Krismer M, Rachbauer F, Eibl G, Stöckl B. Reducing the risk of dislocation after total hip arthroplasty: the effect of orientation of the acetabular component. The Journal of bone and joint surgery British volume. 2005 Jun;87(6).

29. Jolles BM, Zangger P, Leyvraz PF. Factors predisposing to dislocation after primary total hip arthroplasty: a multivariate analysis. The Journal of arthroplasty. 2002 Apr;17(3).

A

Measurement Protocol

Store DICOM files

Store the anonymized DICOM files of the (pre-) and postoperative CT scans in the folder PatientData → Name subfolder: [patientID]

Mimics

If available → Preoperative CT scan

- Import DICOM file preOP CT
- Create the following parts: FemurL_pre, FemurR_pre, PelvisL_pre, PelvisR_pre, Sacrum_pre
- Save As: [patientID]_preop.mcs

Always → Postoperative CT scan

- Import DICOM file postOP CT
- Create the following parts: FemurL_post, FemurR_post, PelvisL_post, PelvisR_post, Sacrum_post
- Segment the LUMiC prosthesis and create parts: LUMiC_cup and Prosthesis_stem
- Save As: [patientID]_postop.mcs

3-matic

If pre- and postoperative CT is available → Alignment

- Copy + paste all pre- and postoperative parts from Mimics to 3Matic
- Use Align → Translate/Rotate to move postOp parts towards preOp parts
  - Main entity: post_PelvisL/R (non affected side)
  - Moving along entities: all other postOp parts
- Use Align → Global registration. Press 'Apply' until perfect registration. Fill in selection as below:
  - Fixed entity: pre_PelvisL/R (non affected side)
  - Moving entity: post_PelvisL/R (non affected side)
  - Moving along entities: all other postOp parts

If only postoperative CT is available → Mirroring and alignment

- Copy + paste all postoperative parts from Mimics to 3Matic
- Use Align → Mirror to mirror the unaffected side (and reconstruct the COR, AV and INCL)
  - Entities: Pelvis_post, Femur_post (non affected side)
  - Mirror plane: World Coordinate System → YZ-plane
- Use Align → Translate/Rotate to move the mirrored parts towards the affected pelvic side
  - Main entity: post_PelvisL/R (non affected side)
  - Moving along entities: post_FemurL/R
- Use Align → Global registration. Press 'Apply' until perfect registration. Fill in selection as below:
  - Fixed entity: post_PelvisL/R (affected side)
  - Moving entity: mirrored post_Pelvis
  - Moving along entities: mirrored post_Femur

→ Check methods section (Chapter 2) for illustrations of landmark positioning

Selection of anatomical landmarks for later determination of the coronal, sagittal and transverse plane

- Hide all postOp parts
- Use Design → Analytical → Point to create points
- Create 2 points on the left and right Anterior Superior Iliac Spine (ASIS). Name: ASIS_L, ASIS_R
- Create 2 points on the left and right pubic tubercles. Name: PT_L, PT_R
- Create 2 points on the sacral crests on the Planning Pelvis. Name: SC_1, SC_2

Selection of landmarks to define acetabular planes

- Hide Pre_Femur
- Create 9 points on the acetabular rim (operated side) and name: AR_1_Pre till AR_9_Pre
- Hide every object except from postOp pelvis (operated side)
- Create 3 points on the acetabular rim and name: AR_1_Post, AR_2_Post and AR_3_Post

Defining COR

- Hide every object except from Pre_Femur (operated side). Use Mark → Wave and mark the femoral head. Use Design → Analytical → Sphere to match a sphere on the marked area (fitting entities: marked triangles). Rename: COR_Pre.
- Repeat the same steps for Post_Femur and name the sphere: COR_Post.

Save and copy points

- Save As: [patientID]_PrePost.mxp
- Select all points and copy with Ctrl + C

Mimics

Check if points are correct

- Open the preOp mcs file. Save as: [patientID]_Pre_Post_points.mcs
- Paste points with Ctrl + V
- Check if the points are correctly positioned in the CT data

Export points to txt files

- Go to File → Export → Txt...
- Click on Analysis and select all points
- Click on Add
- Define File name: points.txt

Python

Calculations

- Open the file calculations.py
- Make sure you have the scikit-spatial toolbox. Otherwise use: ‘pip install scikit-spatial’ (in the Command Prompt)
- Add all patient IDs in the list ‘patient_ids’ (line 230)
- Run the script

The results will be stored in an excel file called patient_deltas.xlsx
The program will not run if this file is already present! So remove or replace it when you run the script twice (e.g. after adding more patient data).

B

Python Calculations

```
#-------------------------------------------------------------------------------

# Name:         Calculations LUMiC
# Purpose:      Comparing COR, anteversion and inclination pre-OP vs post-OP
# Author:       JF van der Geest
# Created:      04-08-2025

#-------------------------------------------------------------------------------
#-------------------------------------------------------------------------------

## Import necessary toolboxes
# first use: pip install scikit-spatial and pip install openpyxl

import numpy as np
import pandas as pd
import sys
from skspatial.objects import Plane, Points

#-------------------------------------------------------------------------------

## Define funtion for calculating plane through 3 points

def define_plane(p1, p2, p3):
    # Determine two vecotrs
    v1 = p2 - p1
    v2 = p3 - p1
    # Find normal vector of the plane using the cross product
    normal_vector = np.cross(v1, v2)
    A, B, C = normal_vector
    # Use one of the points and the normal vector to define the plane equation
    # Ax + By + Cz + D = 0, where [A, B, C] is the normal vector
    D = -np.dot(normal_vector, p1)
    return A, B, C, D, normal_vector

#-------------------------------------------------------------------------------

## Define function to run the calculations for all included patients

def calculate_deltas(patient_folder, patient_id):
    # Define file path
    file_path = f"{patient_folder}/{patient_id}/points.txt"
    print("Performing calculations for patient " + str(patient_id))

    #---------------------------------------------------------------------------
    ## Import points from txt file
    #---------------------------------------------------------------------------
    # Define a dictionary to store the points
    points = {}

    # Open the txt file and read line by line
    with open(file_path, 'r') as file:
        for line in file:
            # Split the line into separate fragments
            txtline = line.split()
            # Check if the line contains one of the necessary points
            if len(txtline) > 0 and txtline[0] in necessary_points:
                # Check if the point already exists in the dictionary
                if txtline[0] in points:
                    print(f"Duplicate point found: {txtline[0]}")
                    sys.exit("Program stopped because duplicate point names are found.")

                # Convert the tuple to NumPy array
                point_array = np.array([float(txtline[1]), float(txtline[2]),
                float(txtline[3])])

                # Create variables for each point
                globals()[txtline[0].replace('_copy', '')] = point_array

                # Add the point to the points dictionary
                points[txtline[0]] = point_array

    # Check if all necessary points are present
    missing_points = [point for point in necessary_points if point not in points]
    if missing_points:
        print("The following necessary points are missing:")
        for point in missing_points:
            print(point)
        sys.exit("Program stopped because necessary points are missing.")
    else:
        print("All necessary points are present.")

    #---------------------------------------------------------------------------
    ## Calculations of anatomical axis and planes
    #---------------------------------------------------------------------------
    # Calculate frontal/coronal plane (FRO)
    # Plane through: ASIS left, ASIS right and midpoint between pubic tubercles
    mean_PT = (PT_L + PT_R) / 2
    FRO_A, FRO_B, FRO_C, FRO_D, n_FRO = define_plane(ASIS_R, ASIS_L, mean_PT)
    print(f"Equation of the frontal/coronal plane (FRO): {FRO_A}x + {FRO_B}y + {FRO_C}z + {FRO_D} = 0")
```

```
# Calculate angle between FRO and CT COR plane
n_FRO_norm = n_FRO / np.linalg.norm(n_FRO)
y_axis = np.array([0, 1, 0])
dot_prod_FRO_y = np.dot(n_FRO_norm, y_axis)
angle_check_COR = np.arccos(np.clip(dot_prod_FRO_y, -1.0, 1.0))
angle_deg_check_COR = np.degrees(angle_check_COR)
print(f"Check angle between FRO plane and CT frontal plane: {angle_deg_check_COR:.2f} degrees")

# Calculate sagittal plane (SAG)
# Plane through: mean of sacral crest points and orthogonal to FRO plane
mean_SC = (SC_1 + SC_2) / 2
# Define vector in sagittal direction (between SC_1 and SC_2)
v_sag = SC_2 - SC_1
v_sag_norm = v_sag / np.linalg.norm(v_sag)
n_SAG = np.cross(n_FRO, v_sag_norm)
n_SAG = n_SAG / np.linalg.norm(n_SAG)
# Define SAG plane
SAG_A, SAG_B, SAG_C = n_SAG
SAG_D = -np.dot(n_SAG, mean_SC)
print(f"Equation of the sagittal plane (SAG): {SAG_A:.3f}x + {SAG_B:.3f}y + {SAG_C:.3f}z + {SAG_D:.3f} = 0")

# Calculate transverse plane (TRA)
n_TRA = np.cross(n_FRO, n_SAG) # Calculate normal vector
n_TRA /= np.linalg.norm(n_TRA) # Normalize the TRA normal vector
TRA_A, TRA_B, TRA_C = n_TRA    # Define variables A, B and C
TRA_D = -np.dot(n_TRA, ASIS_L) # Define D
print(f"Equation of the transverse (TRA) plane: {TRA_A}x + {TRA_B}y + {TRA_C}z + {TRA_D} = 0")

#--------------------------------------------------------------------------
## Calculations of acetabular axis and plane preOP and postOP
#--------------------------------------------------------------------------
# Calculate preOP acetabular plane (ACT_pre)
# Define all points on acetabular rim preOP
points_ACT_pre = Points([AR_1_Pre, AR_2_Pre, AR_3_Pre, AR_4_Pre, AR_5_Pre, AR_6_Pre, AR_7_Pre, AR_8_Pre,
AR_9_Pre])
# Calculate plane
ACT_plane_pre = Plane.best_fit(points_ACT_pre)
# Define normal vector
n_ACT_pre = ACT_plane_pre.normal
ACT_pre_A, ACT_pre_B, ACT_pre_C = n_ACT_pre
# Use points and  normal vector to define D
# Ax + By + Cz + D = 0
ACT_pre_D = -np.dot(n_ACT_pre, ACT_plane_pre.point)
#print(f"Equation of the preOP acetabular plane (ACT_pre): {ACT_pre_A}x + {ACT_pre_B}y + {ACT_pre_C}z +
{ACT_pre_D} = 0")

# Calculate postOP acetabular plane (ACT_post)
ACT_post_A, ACT_post_B, ACT_post_C, ACT_post_D, n_ACT_post = define_plane(AR_1_Post, AR_2_Post, AR_3_Post)
#print(f"Equation of the postOP acetabular plane (ACT_post): {ACT_post_A}x + {ACT_post_B}y + {ACT_post_C}z +
{ACT_post_D} = 0")

#--------------------------------------------------------------------------
## Calculations of anteversion (AV) and inclination (INCL)
#--------------------------------------------------------------------------

# Projection of acetabular axis on FRO (coronal) plane
Proj_ACTonFRO_pre = np.cross(n_FRO, np.cross(n_ACT_pre, n_FRO)) / np.linalg.norm(n_FRO) ** 2
Proj_ACTonFRO_post = np.cross(n_FRO, np.cross(n_ACT_post, n_FRO)) / np.linalg.norm(n_FRO) ** 2

# Radiological Anteversion calculation
# Angle: Acetabular Axis // Acetabular axis projected on FRO (coronal) plane
AV_pre = np.degrees(np.arccos(np.dot(n_ACT_pre, Proj_ACTonFRO_pre) / (np.linalg.norm(n_ACT_pre) *
np.linalg.norm(Proj_ACTonFRO_pre))))
# Correction angle if normal ACT plane is in posterior direction
if AV_pre > 90:
    AV_pre = 180 - AV_pre
AV_post = np.degrees(np.arccos(np.dot(n_ACT_post, Proj_ACTonFRO_post) / (np.linalg.norm(n_ACT_post) *
np.linalg.norm(Proj_ACTonFRO_post))))
if AV_post > 90:
    AV_post = 180 - AV_post
Delta_AV = AV_post - AV_pre
print('Difference anteversion (AV): {:.1f}°'.format(Delta_AV))

# Radiological Inclination calculation
# Angle: Longitudinal axis (Transverse normal vector) // Acetabular axis projected on FRO (coronal) plane
INCL_pre = np.degrees(np.arccos(np.dot(n_TRA, Proj_ACTonFRO_pre) / (np.linalg.norm(n_TRA) *
np.linalg.norm(Proj_ACTonFRO_pre))))
if INCL_pre > 90:
    INCL_pre = 180 - INCL_pre
INCL_post = np.degrees(np.arccos(np.dot(n_TRA, Proj_ACTonFRO_post) / (np.linalg.norm(n_TRA) *
np.linalg.norm(Proj_ACTonFRO_post))))
if INCL_post > 90:
    INCL_post = 180 - INCL_post
Delta_INCL = INCL_post - INCL_pre
print('Difference inclination (INCL): {:.1f}°'.format(Delta_INCL))

#--------------------------------------------------------------------------
## Calculations of displacement COR
#--------------------------------------------------------------------------
```

```
    # Define normal vectors
    y_axis = np.array([0, 1, 0])  # Perfect y-axis

    # Calculate rotation axis (n_FRO to 'perfect y axis')
    v = np.cross(n_FRO, y_axis)

    # Calculate rotation angle
    cos_theta = np.dot(n_FRO, y_axis) / (np.linalg.norm(n_FRO) * np.linalg.norm(y_axis))
    theta = np.arccos(np.clip(cos_theta, -1, 1))

    # Normalize rotation axis
    v /= np.linalg.norm(v)

    # Compute rotation matrix using Rodrigues' rotation formula
    R = np.eye(3) + np.sin(theta) * np.array([[0, -v[2], v[1]],
                                              [v[2], 0, -v[0]],
                                              [-v[1], v[0], 0]]) + \
                   (1 - np.cos(theta)) * np.outer(v, v)

    # Displacement COR in CT coordinate system
    DeltaCOR = COR_Post - COR_Pre
    # Implement rotation matrix to convert to pelvis axis
    DeltaCOR_R = np.dot(R, DeltaCOR)
    # Define medial displacement as positive for prosthesis on the left side
    if COR_Pre[0] > 0:
        DeltaCOR_R[0] = -DeltaCOR_R[0]

    # Calculate vector length (total displacement)
    DeltaCOR_tot = np.linalg.norm(DeltaCOR_R)
    print('Displacement COR: {:.1f} mm'.format(DeltaCOR_tot))


    #---------------------------------------------------------------------------
    ## End calculation, Return outcomes
    #---------------------------------------------------------------------------

    # End statement
    print("Calculations for patient " + str(patient_id) + " are done")
    print('') # Empty line as separation between patients

    # Return outcomes
    return {
        'Patient ID': patient_id,
        'Check_COR' : angle_deg_check_COR,
        'AV pre': AV_pre,
        'AV post': AV_post,
        'Delta AV': Delta_AV,
        'INCL pre': INCL_pre,
        'INCL post': INCL_post,
        'Delta INCL': Delta_INCL,
        'Displacement COR x': DeltaCOR_R[0],
        'Displacement COR y': DeltaCOR_R[1],
        'Displacement COR z': DeltaCOR_R[2],
        'Displacement COR tot': DeltaCOR_tot
    }

#-------------------------------------------------------------------------------

## General settings

# Define necessary points names
necessary_points = ["SC_1_copy", "SC_2_copy", "ASIS_R_copy", "ASIS_L_copy",
                    "PT_L_copy", "PT_R_copy",
                    "AR_1_Pre_copy", "AR_2_Pre_copy", "AR_3_Pre_copy",
                    "AR_4_Pre_copy", "AR_5_Pre_copy", "AR_6_Pre_copy",
                    "AR_7_Pre_copy", "AR_8_Pre_copy", "AR_9_Pre_copy",
                    "AR_1_Post_copy", "AR_2_Post_copy", "AR_3_Post_copy",
                    "COR_Pre_copy", "COR_Post_copy"]

# Define folder and patient IDs
patient_folder = "PatientData" # Fill in correct folder name
patient_ids =  ["xxxxxx", "xxxxxx", "xxxxxx"] # Fill in all patients IDs
#-------------------------------------------------------------------------------

## Storing outcomes for included patients

# Generate empty list to store outcomes
results = []

# Run calculate function for every patient and store results in the list
for patient_id in patient_ids:
    result = calculate_deltas(patient_folder, patient_id)
    results.append(result)

# Save results to Excel file
df = pd.DataFrame(results)
excel_filename = 'patient_deltas.xlsx'
df.to_excel(excel_filename, index=False)
```

C

Comparison of X-ray and CT-based measurements

Postoperative assessment of LUMiC implant positioning: comparing X-ray and CT-based measurements of center of rotation, anteversion and inclination

J.F. (Julia) van der Geest, MSc student Technical Medicine
Delft University of Technology, Erasmus University Medical Center, Leiden University Medical Center
Graduation Internship - Department of Orthopaedics, Leiden University Medical Center

Abstract

Background and objectives: Accurate assessment of acetabular component positioning is essential following pelvic reconstruction with the LUMiC prosthesis, as malpositioning may lead to complications. While computed tomography (CT) is the reference standard for evaluating implant position and orientation, it is not routinely performed due to cost and radiation exposure. This subanalysis of the LUMiC COR study aimed to evaluate the validity of postoperative radiographs as an alternative to CT for position and orientation measurements of the LUMiC prosthesis.
Methods: In this retrospective subanalysis, radiographic measurements of center of rotation (COR), anteversion (AV) and inclination (INCL) were compared to 3D CT-based measurements in patients treated with a LUMiC prosthesis. CT served as the reference standard. Agreement between the two imaging modalities was assessed using paired tests, intraclass correlation coefficients (ICC) and Bland-Altman analysis.
Results: In a cohort of 41 patients, radiographic and CT measurements could be performed in only 17 cases. In this subset, X-ray showed poor agreement with CT. Outliers were present across all parameters.
Conclusion: Radiographic measurements of COR, AV and INCL were often not feasible and showed considerable variability compared to CT. Given these limitations, CT remains the preferred standard.

1. Introduction

Accurate assessment of acetabular component positioning, specifically center of rotation (COR), anteversion (AV) and inclination (INCL), is critical. Deviations in implant positioning may contribute to mechanical complications such as dislocation (1,2). This subanalysis is part of the larger LUMiC COR study, which aims to evaluate the postoperative positioning of the LUMiC prosthesis in patients who have undergone pelvic reconstruction after tumor resection.

Although three-dimensional (3D) computed tomography (CT) is considered the reference standard for evaluating implant orientation, its use is limited in clinical practice due to radiation exposure, cost and availability. In contrast, plain anteroposterior (AP) radiographs are routinely obtained postoperatively, but their accuracy for measuring AV and INCL, particularly in patients with a LUMiC prosthesis, remains uncertain (Appendix E, Literature Study).

Given the limited availability of postoperative CT data in this specific patient population, this subanalysis investigates whether conventional radiographs can serve as a reliable alternative. The aim of this study was to assess the validity of radiographic methods for determining COR, AV and INCL in patients reconstructed with the LUMiC implant, by directly comparing 2D X-ray measurements to 3D CT-derived values.

2. Methods

2.1 Study design

This retrospective single-center subanalysis was conducted at the Leiden University Medical Center (LUMC) and includes a subset of the patient population as described in the study by Evenhuis et al (3). All patients who underwent internal hemipelvectomy with reconstruction using a LUMiC prosthesis between January 2008 and December 2022 in the LUMC were included. The primary aim of this subanalysis was to compare radiographic measurements (COR, AV and INCL) with 3D CT-based values, in order to assess the validity of X-ray as an alternative in settings where CT is unavailable. Ethical approval was granted by the scientific committee of the LUMC (W.24.013/2024-058), which determined that patient informed consent was not required.

2.2 Measurements methods

Measurements on CT were performed using the same semi-automated 3D technique as previously described in the LUMiC COR study (Chapter 3, Methods). These measurements were based on anatomical landmark positioning on CT scans. The first available postoperative CT scan was used for all analyses, following the same inclusion criteria as defined in the LUMiC COR protocol. When available, the preoperative CT scan was used as the anatomical reference for determining the preoperative (native) COR, AV and INCL, measured according to the radiographic definitions as described by Murray (4). In cases where a preoperative scan was not available, the contralateral native hip was mirrored and used as reference, assuming bilateral symmetry (5). COR displacement was assessed in three spatial directions: mediolateral (ML), anteroposterior (AP) and superoinferior (SI), with positive values for medial, posterior and superior translation.

For radiographic measurements, the first postoperative AP pelvic radiograph was used. The contralateral (non-operated) side served as reference for determining preoperative COR, AV and INCL.

COR was measured on X-ray using the method described by Bjarnason et al. (6), which demonstrated high intra- and inter-observer reproducibility in literature (Appendix E, Literature Study). A best-fit circle was drawn over the femoral head or prosthesis head and horizontal and vertical distances from the head center to the vertical midline and inter-ischial line, respectively, were measured (Figure 1).

Displacement of the COR was calculated by comparing the operated side with the contralateral native hip. As illustrated in Figure 1, horizontal (ML, medial) displacement was calculated as the difference between distances "a" and "b" and vertical (SI, cranial) displacement as the difference between distances "d" and "c", corrected for radiographic magnification. The total displacement of the COR was determined by calculating the vector length.

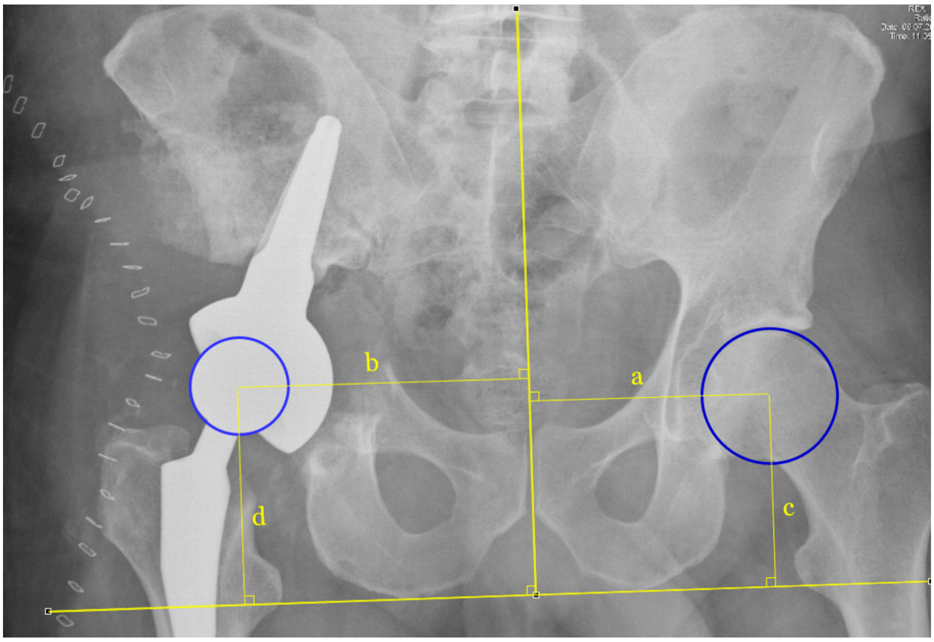

Figure 1. Measurement of the center of rotation (COR) on postoperative anteroposterior radiograph. A best-fit circle was drawn over the femoral or prosthesis head. "a" represents the horizontal distance from the center of the contralateral native femoral head to the vertical midline; "b" represents the horizontal distance from the prosthesis head to the same midline. Distance "c" is the vertical distance from the contralateral head center to the inter-ischial line; "d" is the corresponding distance on the operated side. COR displacement in the mediolateral direction was calculated as *a - b* and in the superoinferior direction as *d - c*, corrected for radiographic magnification.

To correct for magnification, the known diameter of the femoral head prosthesis was used as a calibration reference. A circle was drawn over the prosthetic femoral head to determine its cross-sectional area. From this area, the diameter of the circle was calculated. By comparing the measured diameter on the X-ray with the known actual diameter of the implanted component (retrieved from surgical records), a magnification (or reduction) factor was calculated using the ratio.

Native and prosthetic INCL were measured as the angle between the inter-ischial line and a line along the acetabular rim on the native side (α_1), or the lateral border of the LUMiC cup on the prosthetic side (α_2). Native AV was determined using the method described by Özçelik et al. (7), based on the angle (φ) between lines drawn along the anterior and posterior acetabular walls (Figure 2). These lines were drawn using anatomical landmarks: the anterior wall line intersected the teardrop, while the posterior wall line intersected the lunate sclerosis (Appendix E, Literature Study). The angle between these lines represents native AV.

Prosthetic AV was measured using two commonly applied techniques: Liaw's method and Lewinnek's method, which showed the best reliability and agreement with CT in the literature review (Appendix E). Liaw's method estimates AV by calculating the angle (β) between the long axis of the acetabular component and a line connecting the endpoint of the short axis of the ellipse to the endpoint of the long axis. The anteversion was then calculated using the formula AV = arcsin(tanβ). Lewinnek's method calculates AV using the formula AV = arcsin(D1/D2), where D1 represents the short axis and D2 the long axis of the elliptical projection of the cup (Figure 3).

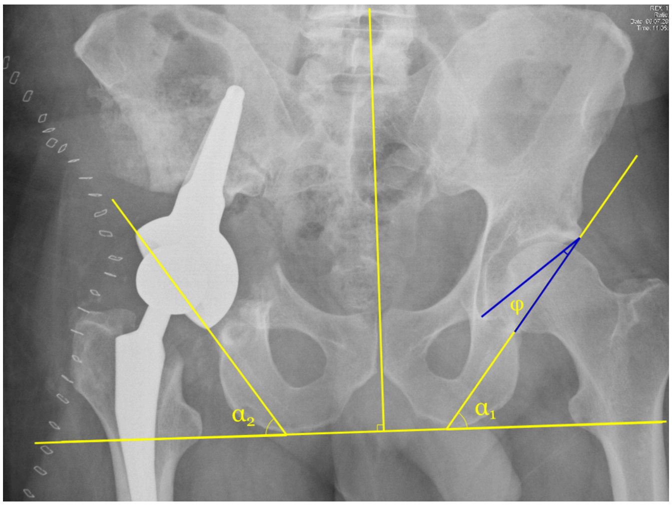

Figure 2. Measurement of inclination (INCL) and anteversion (AV) on preoperative anteroposterior radiographs.
INCL of the native acetabulum (α_1) was measured as the angle between the inter-ischial line and a line along the acetabular rim. Postoperative INCL (α_2) was measured using the lateral border of the LUMiC cup. Pre operative anteversion (φ) was determined using the method described by Özçelik et al., based on the angle between the anterior and posterior acetabular wall lines.

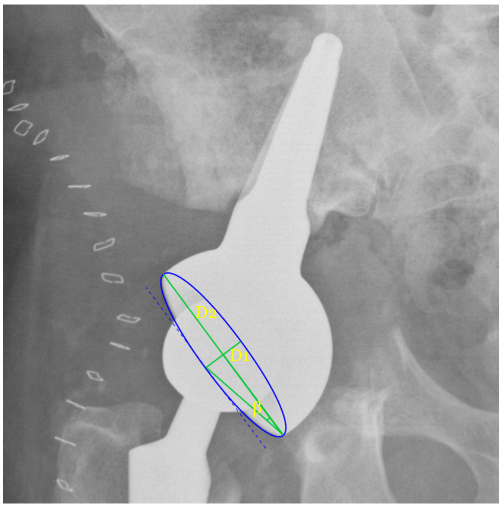

Figure 3. Measurement of prosthetic anteversion (AV) on postoperative radiographs.
Lewinnek AV was calculated using the length of the short axis (D1) to the long axis (D2) of the ellipse. Liaw AV was calculated using angle β.

2.3 Statistics

Descriptive statistics were used to summarize patient characteristics and the availability of imaging data (preoperative CT, postoperative CT and postoperative radiographs). Continuous variables were reported as means with standard deviations (SD) and were compared using unpaired t-tests for normally distributed variables and Mann–Whitney U tests for non-normally distributed variables. Categorical variables were reported as numbers and percentages. The distributions of categorical variables between groups were compared using chi-square tests or Fisher's exact tests. In patients with both CT and postoperative radiograph data available, paired comparisons were performed to assess agreement between COR, AV and INCL measurements obtained from CT and X-ray imaging. Depending on the distribution of differences, comparisons were analyzed using paired t-tests or Wilcoxon signed-rank tests. Normality of the differences was assessed using the Shapiro-Wilk test. To assess inter-modality agreement between CT and X-ray measurements, the intraclass correlation coefficient (ICC) was calculated using a two-way random-effects model (ICC 2,1).

To visually assess agreement between CT-based and X-ray-based measurements, Bland-Altman plots were generated. For each parameter, the difference between the CT and X-ray measurements was plotted against their mean. The mean difference (bias) and the limits of agreement (mean ± 1.96 × standard deviation) were calculated and visualized in each plot.

All analyses were conducted using SPSS version 29.0 (IBM) and Python (matplotlib and scipy). Statistical significance was defined as $p < 0.05$.

3. Results

3.1 Available imaging data

A total of 41 patients received a LUMiC prosthesis at the LUMC between 2008 and 2022. Postoperative X-ray imaging was available for 40 patients, but radiographic measurements were only feasible in 20 cases. In the remaining patients, the large amount of metal obscured the contours of the prosthetic components, making it impossible to fit the necessary geometrical references (example in Figure 4).

Figure 4. Example of a case where the large amount of metal obscured the contours of the prosthetic components.

Postoperative CT scans were available for 32 patients. In 31 cases, measurements could be performed. In one patient, severe pelvic dissociation after tumor resection prevented accurate measurements; this patient was excluded from the analysis. In total, 17 patients had both a postoperative CT scan and an evaluable X-ray, enabling direct comparison between the two imaging modalities.

3.2 Patients characteristics

Table 1 compares the clinical and surgical characteristics of patients with both CT and X-ray measurements to those without measurements. No statistically significant differences were found in age, sex, body mass index (BMI), American Society of Anesthesiologists (ASA) score, type of resection according to the modified Enneking classification (8,9) or postoperative dislocation rates (all $p > 0.05$). These results indicate that the subgroup with imaging data is representative of the overall patient cohort.

Table 1. Summary of patient characteristics: comparison clinical and surgical characteristics between the analyzed subgroup undergoing both X-ray and CT imaging and patients without measurements

Characteristic	Not measured n = 24	X-ray + CT n = 17	p-value
Age at surgery (mean ± SD)	55.4 ± 12.6	47.7 ± 16.7	0.101
Sex, male	10 (41.7)	9 (52.9)	0.537*
Mean BMI (mean kg/m^2 ± SD)	26.0 ± 5.3	26.0 ± 2.9	0.497
ASA score			0.066
ASA1	2 (8.3)	6 (35.3)	
ASA2	17 (70.8)	10 (58.8)	
ASA3	5 (20.8)	1 (5.9)	
Resection type (modified Enneking classification)			0.867
P1b+2	1 (4.2)	2 (11.8)	
P2	11 (45.8)	6 (35.3)	
P2+3	8 (33.3)	6 (35.3)	
P1b+2+3	2 (8.3)	1 (5.9)	
Other	2 (8.3)	2 (11.8)	
Postoperative dislocation	6 (25.0)	3 (17.6)	0.711*

*Values are presented as numbers, with percentages in parentheses, unless otherwise specified. BMI = body mass index, ASA = American Society of Anesthesiologists physical status. *=p-value calculated using Fisher's exact test. SD = standard deviation*

3.3 X-ray vs CT-measurements

In the subgroup of patients with both postoperative CT and radiographs available (n = 17), direct comparisons of COR, AV and INCL measurements were performed (Table 2). Preoperatively, AV measurements showed no significant difference between CT and X-ray, whereas a statistically significant postoperative difference was observed when measured according to Liaw (mean difference = 5.56°, p = 0.040). For INCL, a significant difference was found preoperatively (mean difference = 6.20°, p < 0.001), but not postoperatively.

No statistically significant differences were observed for COR displacements. However, the total COR displacement (2D vector length for X-ray vs. 3D vector length for CT) was, on average, 4.9 mm lower when measured on X-rays, likely reflecting the absence of the AP component in the 2D calculation. Intraclass correlation coefficients (ICCs) ranged from poor to moderate across parameters, with the highest agreement observed for postoperative inclination (ICC = 0.889).

Table 2. Comparison of COR, AV and INCL measurements between CT and X-ray in the paired sample (n = 17).

Characteristic	CT (mean ± SD)	X-ray (mean ± SD)	Mean difference	p-value	ICC
AV pre (°)	16.4 ± 5.2	16.2 ± 3.4	0.27	0.826	0.375
AV post (Liaw, °)	18.0 ± 14.7	12.5 ± 8.4	5.56	0.040*	0.380
AV post (Lewinnek, °)	18.0 ± 14.7	14.7 ± 11.4	3.34	0.611*	0.475
INCL pre (°)	52.5 ± 5.5	46.3 ± 4.0	6.20	<0.001	0.150
INCL post (°)	37.7 ± 19.6	38.5 ± 19.4	-0.89	0.517*	0.889
Delta COR ML (mm)	-8.1 ± 15.9	-8.0 ± 11.4	-0.10	0.487*	0.403
Delta COR SI (mm)	19.2 ± 11.3	18.2 ± 13.0	0.97	0.628	0.786
Delta COR total (mm)	28.1 ± 15.4	23.1 ± 12.2	4.94	0.116	0.588

Values are presented as mean ± standard deviation (SD). P-values are derived from paired t-tests unless indicated otherwise. P-values marked with an asterisk (*) are based on the Wilcoxon signed-rank test due to non-normal distribution of differences. Positive values indicate medial or superior translation of the COR. ML=mediolateral; SI=superoinferior.

3.4 Bland-Altman analysis

The Bland-Altman plots (Figure 5) revealed varying levels of agreement between X-ray and CT measurements across all eight parameters, with outliers present in each plot.

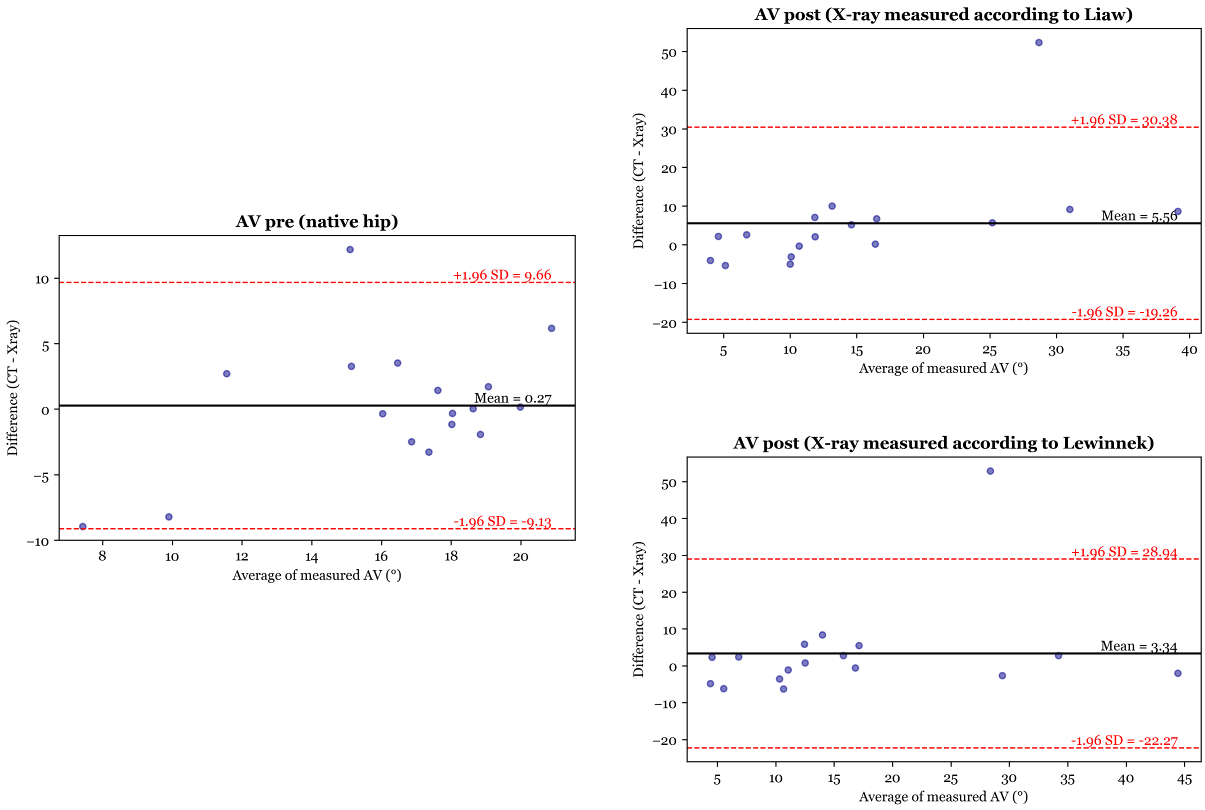

Figure 5a. Bland-Altman plots comparing CT and X-ray measurements. Plots display the agreement between X-ray and CT for preoperative and postoperative acetabular version (AV).

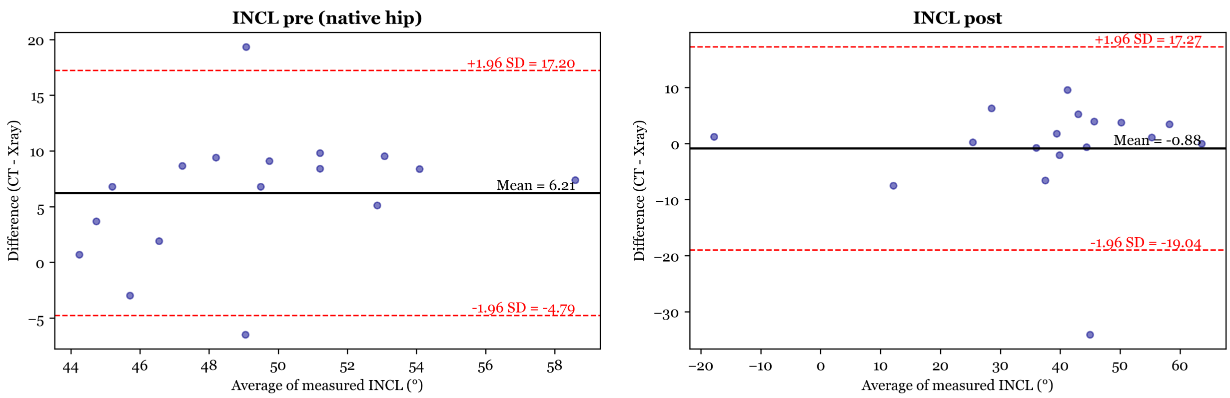

Figure 5b. Bland-Altman plots comparing CT and X-ray measurements. Plots display the agreement between X-ray and CT for preoperative and postoperative inclination (INCL).

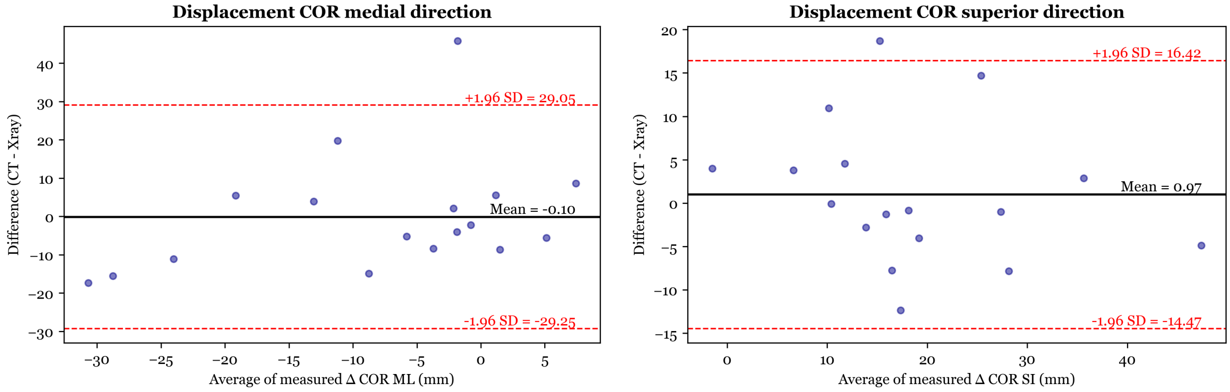

Figure 5c. Bland-Altman plots comparing CT and X-ray measurements. Plots display the agreement between X-ray and CT for centre of rotation (COR) displacement in medial and superior directions.

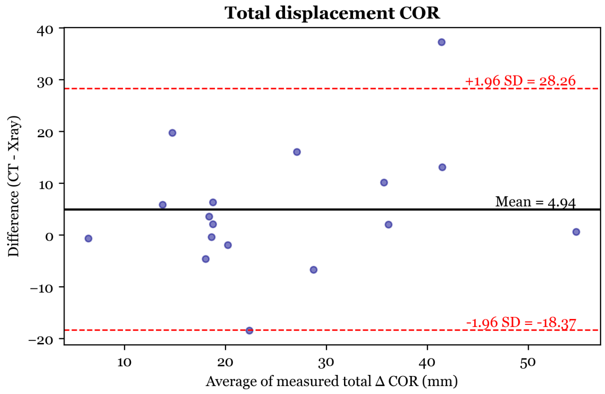

Figure 5d. Bland-Altman plot comparing CT and X-ray measurements. Plots display the agreement between X-ray and CT for total centre of rotation (COR) displacement.

Discussion

This sub-analysis of the LUMiC COR study aimed to assess the validity of postoperative 2D radiographic (X-ray) measurements for evaluating COR, INCL and AV, using 3D CT imaging as reference standard. In the subset of patients with both X-ray and CT data, differences and outliers between modalities were observed. These can partly be explained by differences in reference planes between the two techniques (10). In CT, the coronal plane is often defined according to the anterior pelvic plane (APP), whereas pelvic tilt affects X-ray projections. Using the zy-plane in CT instead of the APP yields a mean difference of 7.3°. With extreme pelvic tilt (up to 22° in one patient), these deviations can be substantial.

AV measurements showed minimal bias preoperatively but significant differences postoperatively. Particularly for small AV angles, X-ray measurements are prone to inaccuracy due to the limited measurable distances and angles. In contrast, CT allows precise assessment in three planes and remains robust in the presence of metal. For COR, X-ray could only assess differences in the ML and SI directions, leading to an underestimation of the total displacement vector compared with CT, which also measures the AP direction. Future research could explore the use of lateral radiographs to capture AP displacement.

A key finding is that radiographic measurements were feasible in only 50% of patients, despite the availability of postoperative X-rays. This reflects a significant practical limitation: large metal implants cause considerable artifacts and projection overlap, making the prosthetic contours difficult to delineate. This not only reduces clinical applicability but may also introduce selection bias, as certain implant positions (e.g., those with larger anteversion) are more easily measurable. Although baseline characteristics were comparable between patients with and without measurable X-rays, suggesting overall comparability between groups, some distortion of representativeness cannot be excluded.

The clinical relevance of the observed differences remains unclear. Previous studies have shown that superolateral displacement of the COR increases total hip joint forces by shortening the moment arm of the hip adductors (11). However, the magnitude of COR, INCL or AV deviation that leads to worse functional outcomes or increased dislocation risk is not yet defined for LUMiC patients. Larger studies with clinical follow-up are needed to establish thresholds for clinical significance.

In addition to the limited feasibility, there are methodological constraints: no repeated measurements were performed and multiple observers were involved, meaning inter- and intra-observer reliability is unknown.

Despite these limitations, the study provides important insights into the limitations of radiographic measurements and supports the use of CT as the preferred modality for accurate assessment of implant positioning in complex reconstructions. Given these findings, systematic use of postoperative CT in patients with LUMiC reconstructions may be justified to evaluate implant positioning, particularly in research settings. Routine CT could improve the accuracy of implant evaluation and facilitate multicenter comparisons. Additionally, the use of low-dose CT protocols or advanced reconstruction techniques (e.g., EOS) may help overcome concerns regarding radiation exposure.

Conclusion

This study demonstrates that standard 2D radiographic measurements of COR, INCL and AV in patients reconstructed with a LUMiC prosthesis differ from CT-based assessments and are frequently infeasible due to metal-induced artifacts. These findings support the use of CT as the preferred imaging modality for accurate evaluation of implant positioning in this patient population. Future research should focus on developing accurate, low-radiation measurement techniques and defining clinically relevant thresholds for implant positioning parameters.

References

1. Qu H, Mou H, Wang K, Tao H, Huang X, Yan X, et al. Risk factor investigation for hip dislocation after periacetabular tumour resection and endoprosthetic reconstruction via thin-slice CT-based 3D model. Bone Joint J. 2022 Oct;104-B(10):1180–8.

2. Wang H, Tang X, Ji T, Yan T, Yang R, Guo W. Risk factors for early dislocation of the hip after periacetabular tumour resection and endoprosthetic reconstruction of the hemipelvis. Bone Joint J. 2021 Feb;103-B(2):382–90.

3. Evenhuis RE, van de Sande MAJ, Fiocco M, Dierselhuis EF, Broekhuis D, Bus MPA, et al. LUMiC Endoprosthetic Reconstruction of Periacetabular Tumor Defects: A Multicenter Follow-up Study. J Bone Joint Surg Am. 2024 Jul 17;106(14):1309–16.

4. Murray DW. The definition and measurement of acetabular orientation. J Bone Joint Surg Br. 1993 Mar;75(2):228–32.

5. Kim SC, Lim YW, Kwon SY, Lee JK, Park IK, Kim YS. Comparative Analysis of Radiographic Hip Joint Geometry Using Measurement Tools on Picture Archiving and Communication System: A Prospective Study of 100 Pelvic Radiographs of Koreans. J Arthroplasty. 2016 Nov;31(11):2597–602.

6. Bjarnason JA, Pripp AH, Reikeras O. Reliability of measures used in radiographic evaluation of the adult hip. Skeletal Radiol. 2015 Jul;44(7):935–9.

7. Özçelik A, Akalın Y, Çalışır C, İnan U, Ömeroğlu H. Definition of a quantitative measurement method for acetabular version in a plain radiograph in the healthy adult hip. Eklem Hastalik Cerrahisi. 2015;26(1):2–5.

8. Bus MPA, Boerhout EJ, Bramer JAM, Dijkstra PDS. Clinical outcome of pedestal cup endoprosthetic reconstruction after resection of a peri-acetabular tumour. Bone Joint J. 2014 Dec;96-B(12):1706–12.

9. Enneking WF, Dunham WK. Resection and reconstruction for primary neoplasms involving the innominate bone. The Journal of bone and joint surgery American volume. 1978 Sep;60(6).

10. Delagrammaticas DE, Alvi HM, Kaat AJ, Sullivan RR, Stover MD, Manning DW. Quantitative Effect of Pelvic Position on Radiographic Assessment of Acetabular Component Position. J Arthroplasty. 2018 Feb;33(2):608–14.e1.

D

Cases

Below are several examples from the study population, illustrating different cases with corresponding screenshots of the 3D models.

Case 110036: Most extreme total COR deviation (60.1 mm)

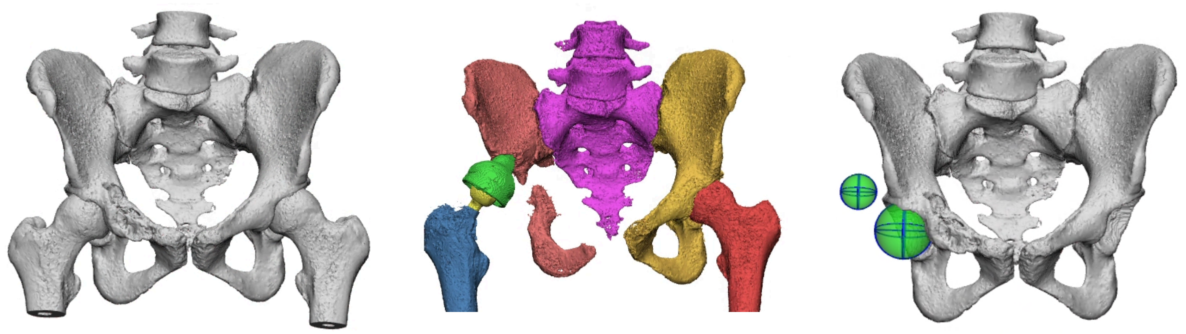

Age: 17
Sex: Female
Diagnosis: Ewing sarcoma
Resection type: P2-P3
Dislocation: No

AV (°)			INCL (°)			Displacement COR (mm)			
pre	post	Δ	pre	post	Δ	ML	AP	SI	total
12.92	2.0	-10.9	62.3	46.0	-16.3	-39.4	-38.1	24.6	60.1

Case 110002: Example COR displacement

Age: 30
Sex: Female
Diagnosis: Metastasis
Resection type: P1-P2
Dislocation: No

AV (°)			INCL (°)			Displacement COR (mm)			
pre	post	Δ	pre	post	Δ	ML	AP	SI	total
17.4	8.0	-9.4	47.5	44.1	-3.5	-36.5	-15.9	26.7	48.0

Case 110007: Large COR displacement

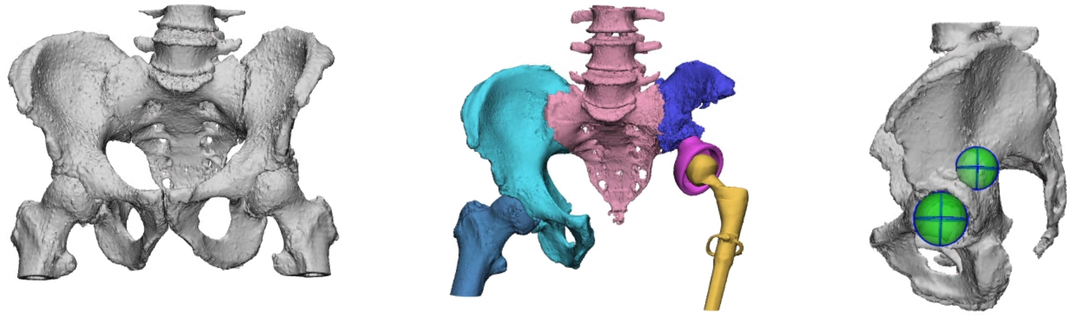

Age: 59
Sex: Male
Diagnosis: Chondrosarcoma
Resection type: P1-P2-P3
Dislocation: No

AV (°)			INCL (°)			Displacement COR (mm)			
pre	post	Δ	pre	post	Δ	ML	AP	SI	total
18.3	28.1	9.7	48.6	63.6	15.0	-16.4	27.2	45.0	55.0

Case 110028: Large COR displacement

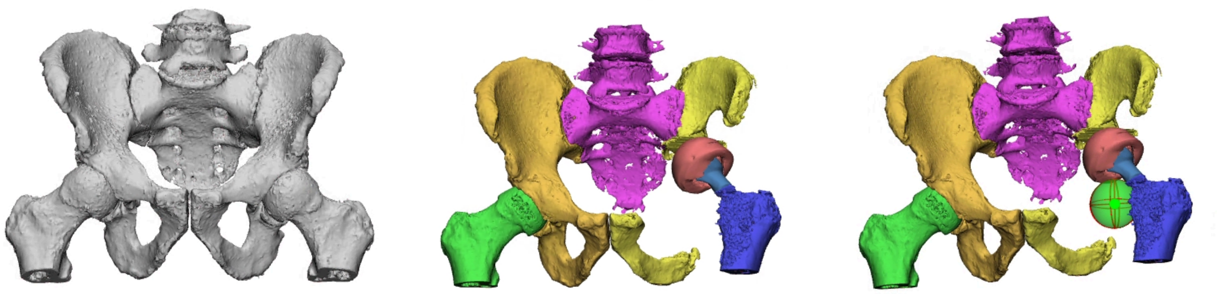

Age: 28
Sex: Male
Diagnosis: Chondrosarcoma
Resection type: P2-P3
Dislocation: No

AV (°)			INCL (°)			Displacement COR (mm)			
pre	post	Δ	pre	post	Δ	ML	AP	SI	total
24.7	26.8	2.2	58.3	41.2	-17.1	-4.6	17.2	43.5	47.0

Case 140012: Superior COR displacement

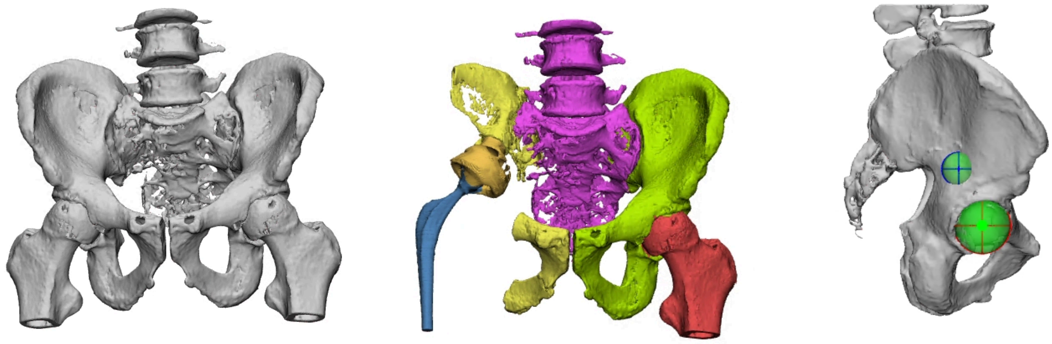

Age: 72

Sex: Male

Diagnosis: Metastasis

Resection type: P1-P2-P3

Dislocation: No

AV (°)			INCL (°)			Displacement COR (mm)			
pre	post	Δ	pre	post	Δ	ML	AP	SI	total
19.1	7.5	-11.6	55.0	34.5	-20.5	-3.6	21.4	48.2	52.8

Case 150006: Dislocation

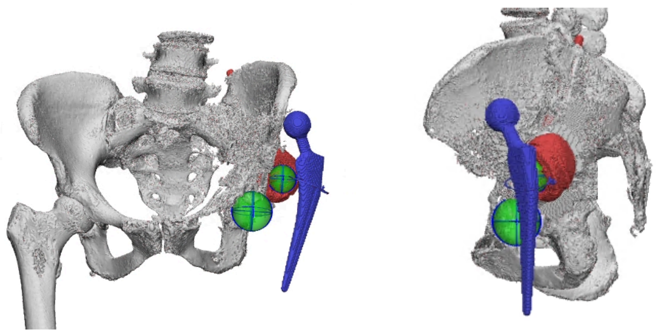

Age: 74

Sex: Female

Diagnosis: Metastasis

Resection type: P1-P2

Dislocation: Yes

AV (°)			INCL (°)			Displacement COR (mm)			
pre	post	Δ	pre	post	Δ	ML	AP	SI	total
23.0	50.8	27.8	61.0	74.4	13.3	-27.4	26.4	34.2	51.2

Case 110013: Pelvic dissociation

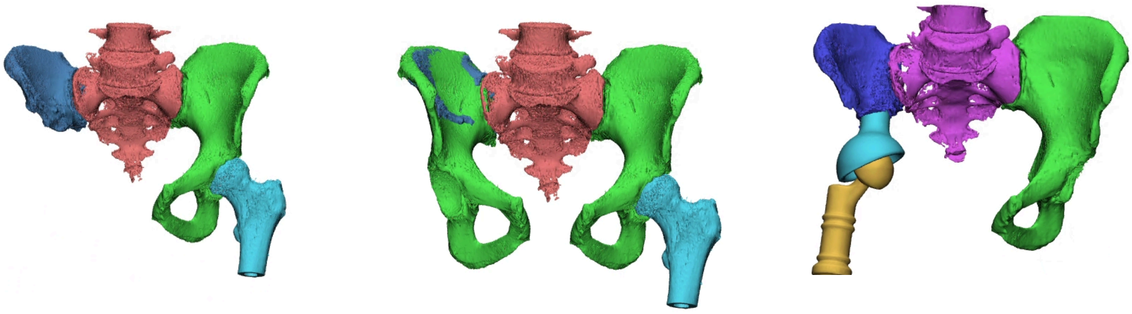

Age: 56
Sex: Female
Diagnosis: Chondrosarcoma
Resection type: P2-P3
Dislocation: No

Not included in analysis

E

Literature Review

Analysis of measurement techniques in pelvic imaging
A Literature Review

J.F. (Julia) van der Geest, MSc student Technical Medicine
Leiden University Medical Center, Delft University of Technology, Erasmus University Medical Center Rotterdam
Graduation Internship - Department of Orthopaedics, Leiden University Medical Center

Abstract

Background and objectives: This review is part of a study investigating postoperative positioning of the LUMiC prosthesis. Given the limited availability of CT imaging and the widespread use of radiographs, it is essential to assess whether reliable measurements of the center of rotation (COR), anteversion (AV) and inclination (INCL) can be obtained from X-rays. This review evaluates available measurement techniques and compares their accuracy and reliability between CT and X-ray modalities.

Methods: A comprehensive literature review of studies was conducted using PubMed. Articles describing X-ray and CT-based techniques for pelvic parameter measurements were screened. The primary focus was on studies evaluating reliability, validity, interobserver and intraobserver variability of these techniques.

Results: 3D CT imaging consistently demonstrated superior accuracy in measuring COR, AV and INCL. High inter- and intraobserver reproducibility was reported for both X-ray and 3D CT methods, although CT-based techniques achieved higher intraclass correlation coefficient (ICC) values and smaller measurement errors. Variability among 2D methods was notable, but newer 2D-3D registration methods showed improved accuracy.

Conclusion: While 2D radiographic techniques remain reliable, 3D CT methods provide greater accuracy. Integration of 2D-3D registration techniques may enhance reliability and accuracy in postoperative evaluations. The choice of method should depend on the required precision and available resources. However, the applicability of these findings to patients with a LUMiC prosthesis remains uncertain.

Keywords

"Measurements methods", "Acetabular orientation", "Hip center of rotation", "Computed Tomography", "Radiographs"

1. Introduction

This literature review was conducted in the context of the LUMiC COR study, which aims to evaluate the position of the hip joint's center of rotation (COR), anteversion (AV) and inclination (INCL) in patients who have received a LUMiC prosthesis.

Accurate positioning of hip joint prostheses is critical for minimizing post-surgical complications (1,2). Proper implant placement directly influences the range of motion, reduces the risk of dislocation and decreases implant wear. Additionally, correct positioning contributes to improved functional outcomes and prolonged implant survival (3–7). Key metrics used to evaluate implant positioning include the COR, AV and INCL of the acetabular component.

Traditionally, these measurements have been derived from plain radiographs, given their widespread availability and low cost. In recent years, computed tomography (CT) imaging has enabled more detailed, three-dimensional (3D) assessment of implant positioning and allows for the incorporation of pelvic tilt. Although CT is considered more precise, there is no universally accepted gold standard for measuring COR, AV and INCL. Therefore, measurement outcomes may vary depending on the method used.

Due to the rarity of the LUMiC prosthesis, postoperative CT scans are available for only a limited number of patients, whereas standard radiographs are available for nearly all. To assess potential risks associated with altered COR, AV and INCL, it is essential to include as many patients as possible. While CT is generally preferred due to its 3D imaging capabilities, it is important to determine whether comparable measurements can be reliably derived from standard two-dimensional (2D) radiographs.

A major challenge lies in direct comparison between radiographic and CT-based measurements. Specifically, the extrapolation of 3D parameters from 2D radiographs introduces inherent technical limitations. For instance, only the projected 2D location of the COR can be determined on X-ray. Similarly, INCL is generally more reliably assessed than AV, which involves rotation around an axis not easily visualized in 2D imaging. Differences in coordinate systems and reference planes between imaging modalities further complicate direct comparison.

Therefore, the aim of this literature review is twofold: 1) to provide an overview of the existing methods for measuring COR, AV and INCL using X-ray and CT, in order to identify the most accurate and reliable techniques and 2) to investigate how measurement outcomes from X-ray imaging compare to those from CT.

2. Methods

2.1 Literature search

A comprehensive literature search was conducted on October 9th, 2024 using PubMed to identify studies related to acetabular orientation and radiological techniques for hip joint assessments. The search strategy combined Medical Subject Headings (MeSH) terms and free-text terms to capture a broad spectrum of relevant articles. Key search terms included combinations such as "acetabular orientation", "anteversion", "center of rotation", "inclination", "radiograph", "X-ray", "computed tomography", "accuracy" and "reliability". The detailed search string is provided in the Appendix.

The search was designed to identify studies evaluating radiological methods, including AP radiograph and 3D CT imaging, for determining acetabular orientation using COR, AV and INCL with a focus on the reliability, validity and accuracy of these methods. Only studies reporting the radiographic AV and INCL, as outlined by Murray, were included (8). According to Murray, radiographic AV is defined as the angle between the acetabular axis and the coronal plane, while radiographic INCL is defined as the angle between the longitudinal axis and the acetabular axis as projected onto the coronal plane.

Studies were included if they involved measurements in native hip joints and/or hips with a total hip arthroplasty (THA). In addition to the PubMed search, the reference lists and citation lists of the selected articles were screened to identify any additional relevant studies that may not have been captured during the database search. The review was limited to articles written in English.

2.2 Study selection

Titles and abstracts of retrieved articles were screened to assess their relevance. Full-text articles of potentially relevant studies were obtained and further evaluated for eligibility based on the following inclusion and exclusion criteria.

Inclusion criteria:

- Studies describing techniques for measuring COR, AV and INCL using (AP) X-ray, 3D CT or 2D-3D matching.
- Studies where the technique used was clearly and thoroughly described.
- Studies reporting outcome measures such as intraclass correlation coefficient (ICC) or comparisons with a gold standard for accuracy.
- Studies using radiographic INCL and AV as defined by Murray.

Exclusion criteria:

- Studies using methods based primarily on CT slice measurements (2D-CT).
- Studies focusing on perioperative measurement techniques.

Only studies meeting all inclusion criteria and none of the exclusion criteria were included in the final review.

2.3 Data extraction

From each eligible study, the following data were extracted:

- Study population: characteristics of the patients included in the study.
- Measurement method: detailed description of the imaging techniques and procedures used for measuring COR, AV and INCL.
- Reliability and validity metrics: ICC and other reliability measures, as well as comparisons with gold-standard methods (e.g., mean differences or measures of accuracy). ICC values were characterized as slight (0.00 to 0.20), fair (0.21 to 0.40), moderate (0.41 to 0.60), substantial (0.61 to 0.80) and almost perfect (> 0.80), consistent with existing literature (9).

3. Results

A total of 504 studies were retrieved using the predefined search algorithm as described in the methods section. After screening titles and abstracts, 392 studies were excluded as they did not meet the inclusion criteria, leaving 112 articles for full-text analysis. Of these, 89 articles were excluded for specific reasons: 28 studies lacked validation, 25 did not report appropriate outcome measures,
23 relied on 2D slice measurements and 13 provided insufficient methodological explanations. Additionally, 2 studies were identified through reference and citation searching. In total, 25 articles met all inclusion criteria and were included in the literature review. The screening and selection process is illustrated in the flow diagram (Figure 1).

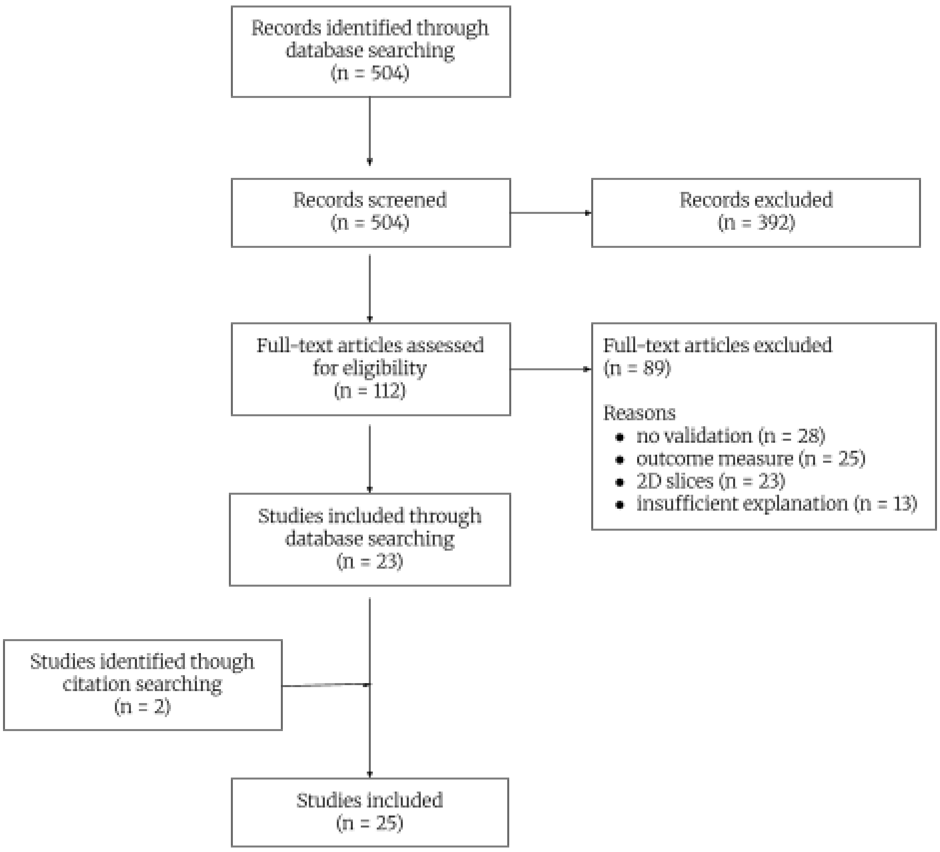

Figure 1. Flow diagram, illustrating the process of literature selection and inclusion in this review

3.1 X-ray: determination of the center of rotation

Bjarnason et al. assessed the reliability of determining the COR using X-rays in 35 patients prior to THA, focusing on unilateral measurements (10). Patients with distorted anatomy, such as femoral head necrosis, were excluded to ensure measurement consistency. The study employed the inter-ischial line and a perpendicular line through the center of the pubic symphysis as reference points. The COR was determined by fitting a circle to the femoral head and the acetabular border. Measurements included the distance between the vertical midline and the COR (denoted as A) and the distance between the horizontal line and the COR (denoted as E), as depicted in Figure 2. Intra- and inter-observer reliability were almost perfect, with ICCs of 0.99. The 95% confidence intervals ranged from 0.981 to 0.999 for intra-observer measurements and from 0.977 to 0.998 for inter-observer measurements.

Schofer et al. evaluated six methods for determining the COR in cases with abnormal femoral head geometry, using a dataset of 230 hip joints from 115 healthy individuals for validation of the method (11). These methods included those described by Fessy, John and Fisher, Pierchon and Ranawat (12–15). None of these methods relied on drawing a circle over the femoral head. Instead they determined the COR by analyzing pelvic proportions and anatomical landmarks, using specific formulas.

Among the six methods, the approach described by Fessy showed the best performance, with the smallest mean deviation from the true anatomical center, measuring 1.69 ± 0.87 mm. The Fessy method calculates the vertical (Y) and horizontal (X) positions of the COR relative to the distal end of the acetabular teardrop. The vertical distance is determined using the equation $Y = 0.204L-0.794$, where L is the distance between lines connecting the inferior edges of the sacroiliac joints and the acetabular teardrops (Figure 3). To calculate the horizontal distance (X), Fessy's method uses Koehler's line as a reference. For men, X is defined by the formula $X=0.093I+33.195$, where I is the distance along Koehler's line. For women, X is correlated with the calculated Y and determined by $X=0.284Y+29.016$.

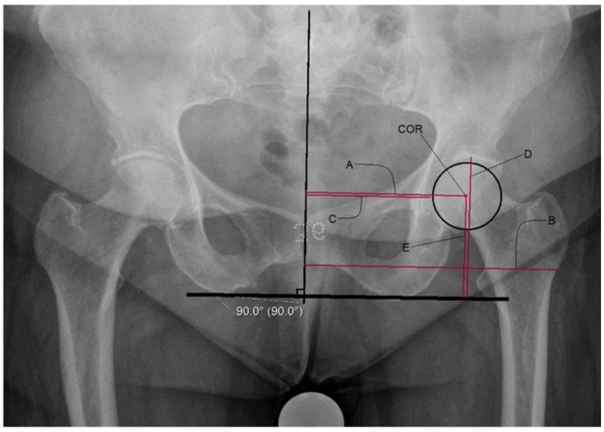

Figure 2. Measurement method COR Bjarnasson et al. Reference lines are in bold black perpendicular to each other. A=Distance between vertical midline and COR. E= Distance between horizontal line and COR.

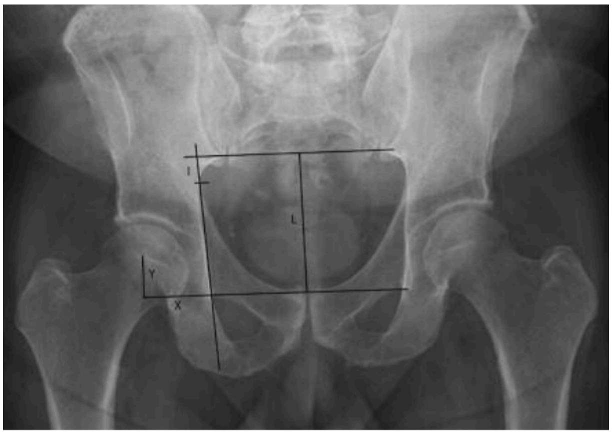

Figure 3. Measurement method COR Fessy et al.

3.2 X-ray: determination of the anteversion

Anteversion measurement in native hips

AV determination has been studied extensively across various radiographic techniques, primarily in the context of THA. Most studies compare these techniques against CT-derived measurements, with multiple methods evaluated for reliability, validity and accuracy. Only one study, conducted by Özçelik et al., investigated AV measurements in native hips rather than after THA (16). Özçelik et al. assessed the AV angle of the acetabulum in 78 native hips from 39 patients without osteoarthritis-related changes. Using AP pelvic radiographs, AV angle was measured as the angle formed between the anterior and posterior acetabular wall lines on the radiograph (Figure 4). This angle was assigned a negative value if the anterior wall line was lateral to the posterior wall line. Measurements were compared with CT-slices as the reference standard. The study reported high intra- and interobserver reliability, with mean intraobserver differences of 1.3° (0–5°) and 1.5° (0–6°) and interobserver difference of 1.4° (0–5°). When compared to CT, the mean difference was 2.5° (0–6°), with 89% of the hips showing differences between 0 and 4°.

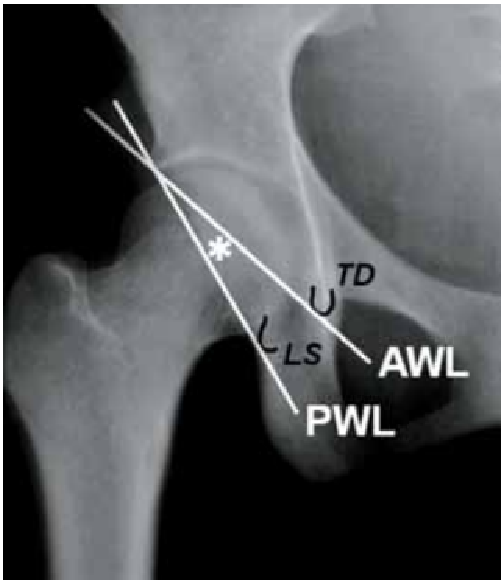

Figure 4. Measurement of acetabular anteversion in a plain anteroposterior radiograph. AWL=anterior wall line; PWL=posterior wall line; TD=teardrop; LS=lunate sclerosis; *=acetabular anteversion angle.

Anteversion measurement in THA

Numerous studies have evaluated the reliability (intra- and inter-observer consistency) and validity of various radiographic methods used to measure acetabular AV after THA, as AV is considered most challenging to measure accurately on plain radiographs due to the complexity of projecting a three-dimensional angle onto a two-dimensional image. Methods assessed in the reviewed studies include the measurement techniques from Lewinnek (4), Widmer (17), Hassan (18), Ackland (19), Liaw (20), Pradhan (21) and McLaren (22). Most methods were validated against reference standards such as CT.

The following studies were included in this review:

1. Nho et al. (23) compared five methods (Lewinnek, Widmer, Hassan, Ackland and Liaw) in a population of 36 THA patients, with three examiners assessing inter-observer reliability and one examiner performing intra-observer reliability with a three-week interval. CT slices served as the reference standard.
2. Lee et al. (24) used a custom-made validation model to compare six methods (Lewinnek, Widmer, Hassan, Ackland, Liaw and Pradhan). AV angles were adjusted from 0° to 30° in 5° increments, while INCL angles were varied from 10° to 70° in 10° increments. For each combination of AV and INCL, radiographs were generated and subsequently measured by two orthopedic surgeons. These measurements were repeated two months later to assess intra-observer reliability.
3. Alzohiry et al. (25) evaluated five methods (Lewinnek, Widmer, Hassan, Ackland and Liaw) in two distinct groups: 37 uncemented cups and 23 cemented cups, making a total of 60 THA patients. CT slices were used as the reference standard.

4. Park et al. (26) analyzed five methods (Lewinnek, Widmer, Hassan, Ackland and Liaw) in 71 THA patients. The PolyWare program (Draftware Developers Inc., Vevay, Indiana), which reconstructs acetabular components on AP radiographs, served as the reference standard. Inter-observer reliability was assessed by three examiners, with intra-observer reliability measured by one examiner after two weeks.
5. Nomura et al. (27) evaluated four methods (Lewinnek, Widmer, Liaw and Pradhan) in 84 THA patients, using CT slices as the reference standard. Four examiners assessed inter-observer reliability and one examiner repeated measurements three times at two-week intervals.
6. Marx et al. (28) evaluated five methods (Widmer, Hassan, Ackland, Pradhan and McLaren) in 42 THA patients. CT-based 3D reconstructions served as the reference, with no intra- or inter-observer reliability assessed.
7. Shin et al. (29) focused on the Liaw method using PolyWare as the reference standard in 551 THAs. PolyWare software was used as a reference standard. Inter-observer reliability was assessed with three examiners, while intra-observer reliability involved one examiner repeating measurements three times at two-week intervals.
8. Manjunath et al. (30) assessed five methods (Lewinnek, Widmer, Hassan, Liaw and Pradhan) in 30 hips (25 patients), using CT slices as the control. For intra-observer reliability, one observer measured AV twice for all methods within a four-week interval. For inter-observer reliability, three observers independently evaluated the measurements.

Tables 1 and 2 summarize ICC values, showing almost perfect reliability for all methods. The results of comparative analyses are summarized in Table 3. The table highlights the deviations of each method from reference standards such as CT slices, PolyWare and 3D CT models. Statistically significant differences ($p < 0.05$, highlighted in blue) reveal variability in accuracy across methods. The Liaw and Lewinnek methods demonstrated small deviations from reference standards, suggesting relatively high validity. In contrast, the Widmer, Hassan, Pradhan, Ackland and McLaren methods often displayed substantial discrepancies.

Table 1. Intra-observer reliability (ICC) of acetabular anteversion measurements on X-ray after THA, using various radiographic methods.

Study	Lewinnek	Widmer	Hassan	Ackland	Liaw	Pradhan
Nho	0.954	0.938	0.920	0.914	0.915	
Lee	0.916	0.933	0.899	0.913	0.908	0.934
Park	0.938	0.923	0.953	0.936	0.933	
Normura	0.930	0.925			0.922	0.913
Shin					0.957	
Manjunath	0.920	0.916	0.904		0.954	0.920

Table 2. Inter-observer reliability (ICC) of acetabular anteversion measurements on X-ray after THA, using various radiographic methods.

Study	Lewinnek	Widmer	Hassan	Ackland	Liaw	Pradhan
Nho	0.943	0.961	0.936	0.865	0.929	
Lee	0.937	0.928	0.902	0.886	0.887	0.938
Park	0.927	0.954	0.928	0.923	0.925	
Normura	0.946	0.944			0.929	0.923
Shin					0.917	
Manjunath	0.938	0.942	0.908		0.962	0.914

Table 3. Mean differences in acetabular anteversion measurements compared to reference methods (CT, 3D models or software) after THA

Study	Reference	Lewinnek	Widmer	Hassan	Ackland	Liaw	Pradhan	McLaren
Nho	CT slices	0.10	**-7.66**	−0.69	**-11.14**	1.68		
Lee	Model	2.84	-7.10	**-12.95**	**-10.15**	2.52	1.62	
Alzohiry (UC)	CT slices	0.20	**2.31**	0.02	**2.17**	0.20		
Alzohiry (CEM)	CT slices	0.23	**1.93**	0.16	**1.22**	0.28		
Park	PolyWare	**-2.21**	**5.00**	**-2.13**	**1.43**	-0.33		
Nomura	CT slices	**-4.6**	−0.9			**-4.1**	**-5.3**	
Marx	3D model CT		**-6.4**	**-14.4**	**-14.3**		**-14.5**	**-14.5**
Shin	PolyWare					1.06		
Manjunath	CT slices	4.330	**6.840**	4.880		4.390	6.220	

Values represent mean differences (in degrees) between radiographic methods and the reference standard. Statistically significant differences ($p < 0.05$) are shown in bold blue. UC = uncemented; CEM = cemented.

Liaw's and Lewinnek's methods are widely used for assessing acetabular AV on radiographs due to their accuracy and simplicity. Liaw's method refines the measurement by incorporating the angle (β) formed between the long axis of the acetabular component (AB) and a line connecting the top point of the ellipse with the endpoint of the long axis (AC). The formula for this method is AV = arcsin(tanβ), Figure 5a. In comparison, Lewinnek's method calculates AV using the formula AV = arcsin(D1/D2). D1 represents the short axis of the elliptical projection of the acetabular component and D2 reflects the long axis of the ellipse, Figure 5b.

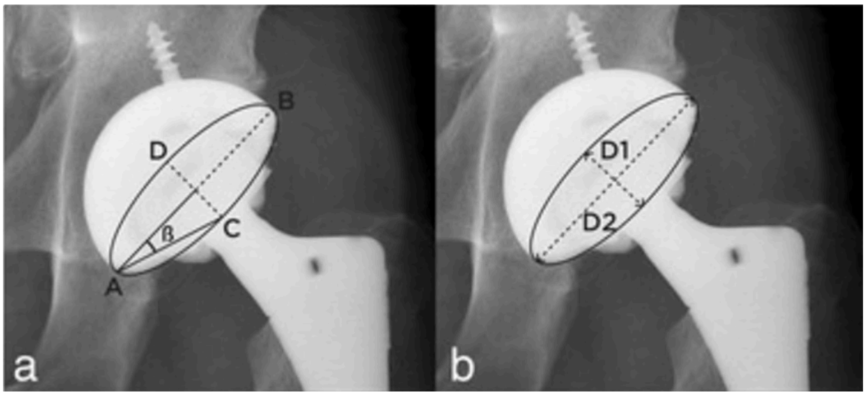

Figure 5. Measurement of acetabular anteversion in a plain anteroposterior radiograph using (a) Liaw's or (b) Lewinnek's method.

Inclination measurement

No studies were identified that specifically investigated the variability or reliability of INCL measurements using AP radiographs. Additionally, no comparative studies were found that assessed the accuracy or consistency of different techniques for measuring INCL on AP radiographs.

3.3 3D analysis

Reference planes and anatomical landmarks

All included studies used the anterior pelvic plane (APP) as a reference frame. Originally introduced by Lewinnek et al., the APP is defined by the most anterior points of the bilateral anterior superior iliac spines (ASIS) and the midpoint of the pubic tubercles (PT), establishing the frontal plane for orientation (4). Additional reference planes include the mid-sagittal plane (MSP), which passes through the midpoint between the ASISs with a normal vector and the transverse plane, orthogonal to both the APP and MSP.

3D measurements

Different studies were included to summarize 3D measurement techniques. A summary of all studies is displayed in Table 4.

1. Zhang et al. (31) analyzed 100 subjects with non-orthopedic CT scans (1 mm slices) to assess 3D acetabular orientation. Segmentation involved approximately 20 rim points, generating a best-fit circle of the acetabular opening via least-squares methods. The acetabular axis was perpendicular to the circle and ICC values >0.999 confirmed excellent intra- and interobserver reliability for measuring AV and INCL.
2. Chen et al. (32) employed a semi-automated 3D CT technique using four APP points and 20 rim points that were optimized by an algorithm. The algorithm was evaluated in 88 non orthopaedic subjects. Reliability for AV and INCL was high, with intra-rater ICCs >0.999 and inter-rater ICCs >0.996.
3. Henckel et al. (33) investigated the accuracy of acetabular implant measurements using CT scans of two artificial pelvis models (Sawbone), scanned three times with varying tilts (0°, 10°, 20°). For determining acetabular orientation 20 rim points were placed. ICCs >0.9 for INCL and AV were achieved, demonstrating high precision.
4. Barlow et al. (34) assessed 258 hemipelvises (129 subjects) with non-orthopedic CT scans. They compared 2D AV from axial slices against 3D CT. Acetabular axis was defined by marking the acetabular rim which was modeled as a circle afterwards. The mean 2D-3D AV difference was 5.8° ± 4.9° ($p < 0.0001$).
5. Park et al. (35) compared 2D and 3D CT in 96 non-orthopedic patients using APP and sphere-fitting (~20 points on rim) methods. Results showed significant discrepancies between 2D and 3D INCL (42° vs. 53°) and AV (19° vs. 15°). ICCs revealed 3D CT's superior reproducibility (intra-rater ICC: INCL = 0.98, AV = 0.99 vs. 2D: INCL = 0.55, AV = 0.81).
6. Hart et al. (36) studied 49 patients with metal-on-metal (MoM) implants using low-radiation CT and radiographs. 20 landmarks were placed on the cup for determining the acetabular axis. The study identified a mean INCL difference of 4.1° and AV differences of 14.2° (statistically significant). The ICCs for the 3D CT method were 0.99 for INCL and 0.94 for AV.
7. Lu et al. (37) analyzed 60 THA patients, comparing the Lewinneck radiographic method against 3D CT. For the 3D method, landmarks included the ASIS, PT and three evenly distributed points on the acetabular cup. INCL differences were statistically significant (2.32° ± 1.83°, $p < 0.05$). AV differences between the two methods were non-significant (0.55° ± 3.1°).
8. Lubovsky et al. (38) compared 3D CT and CT-generated AP pelvic radiographs in 38 non-orthopedic patients. Landmarks for 3D included APP and ≥16 acetabular rim points. Results showed significant differences in INCL (3D: 46.1° ± 9.4° vs. radiograph: 57.8° ± 4.0°). Radiographic AV was not analyzed.

2D-3D registration vs 3D CT

2D-3D registration techniques integrate conventional 2D radiographs with 3D pre- or postoperative models or statistical shape models, enabling accurate measurement of prosthetic positions and native acetabular parameters.

1. Nees et al. (39) evaluated 7 patients with severe acetabular defects (Paprosky ≥ Type IIIA) using proprietary software. Postoperative 2D radiographs were aligned with preoperative 3D CT plans. The 2D-3D registration was compared with postoperative 3D CT. The mean deviations were 1.4 mm in the craniocaudal direction and 2.7 mm in the lateromedial direction for the COR, 3.6° for AV and 0.7° for INCL.
2. Craiovan et al. (40) used a statistical shape model-based 2D-3D registration to analyze 21 THA patients. For determining the acetabular axis 3 landmarks were placed on the cup. The mean deviation of 2D-3D from 3D CT was -1.4° ± 1.8° for INCL. AV was not reported due to the use of anatomical definitions.
3. Zheng et al. (41) studied 10 cadavers with 20 THAs using the HipMatch hybrid 2D-3D system. Preoperative CT was registered to 2D radiographs, resulting in INCL deviations of 1.0° ± 0.7° and high reliability (ICC >0.96).
4. Weber et al. (42) analyzed 11 Paprosky type II defects using a 2D-3D overlay approach. Compared to 3D CT, deviations were minimal (INCL: 1.1° ± 1.7°; AV: -2.6° ± 1.3°; COR: 1.3 mm ± 3.5 mm).
5. Zheng et al. (43) tested a 2D-3D registration method using statistical shape modeling on 31 THAs (29 patients). Landmarks included APP and three points on the cup rim to define orientation. Mean accuracy was excellent for INCL (0.4° ± 1.8°, range -2.6° to 3.3°) and AV (0.6° ± 1.5°, range -2.0° to 3.9°). Both inter- and intraobserver ICCs exceeded 0.96 for INCL and AV.
6. Steppacher et al. (44) validated the 2D-3D registration program HipMatch in 25 THA patients. For calculating AV and INCL 6 points were placed on the cup opening face. INCL deviations averaged 1.7° ± 1.7° and AV deviations 0.9° ± 2.8°. Interobserver ICCs were excellent for both INCL (0.96) and AV (0.95).

Table 4. Overview of studies comparing 2D, 2D-3D matching and 3D CT-based techniques for acetabular orientation assessment. Summary of subject characteristics, methods, anatomical landmarks and reported outcomes, including mean differences in center of rotation (COR), anteversion (AV), inclination (INCL), and intra-/inter-observer reliability (ICC) where available.

Study	Subjects (n)	Indication	Method	Landmarks	COR (mm)	AV (°)	INCL (°)	ICC
Zhang (2017)	100	Native hip Non-ortho	3D	APP, 20 rim points, best-fit circle	NA	only ICC	only ICC	>0.999 (INTRA/ INTER)
Chen (2017)	88	Native hip Non-ortho	3D	APP, 20 rim points	NA	only ICC	only ICC	INTRA >0.999, INTER >0.996
Henckel (2023)	2	Sawbone with implant	3D (varying tilt)	APP, 20 rim points	NA	only ICC	only ICC	>0.9 (INCL/AV)
Barlow (2022)	129 (258 hips)	Native hip Non-ortho	2D vs. 3D	APP, marking acetabular rim	NA	5.8 ± 4.9	NA	NA
Park (2016)	96	Native hip Non-ortho	2D vs. 3D	APP, 20 rim points	NA	2D: 19; 3D: 15.0	2D: 42; 3D: 53	2D: 0.55–0.81; 3D: >0.98
Hart (2010)	49	MoM implants	3D CT vs. X-ray	APP, 20 rim points	NA	14.2	4.1	INCL = 0.99, AV = 0.94
Lu (2018)	60	Post-THA	2D vs. 3D	APP, 3 cup points	NA	0.55 ± 3.1	2.32 ± 1.83	NA
Nees (2023)	7	Paprosky IIIA defects	2D-3D vs. 3D	Proprietary software	1.4 (CC), 2.7 (LM)	3.6	0.7	NA
Craiovan (2014)	21	Post-THA	2D-3D vs. 3D	APP, 3 rim points	NA	NA	-1.4 ± 1.8	NA
Zheng (2010)	10 (20 hips)	Cadavers (THA)	2D-3D vs. 3D	HipMatch hybrid software	NA	NA	1.0 ± 0.7	>0.96 (INTRA/ INTER)
Weber (2018)	11	Paprosky II defects	2D-3D vs. 3D	Proprietary overlay system	1.3 ± 3.5	-2.6 ± 1.3	1.1 ± 1.7	NA
Zheng (2011)	29 (31 hips)	Postoperative THA	2D-3D vs. 3D	APP, 3 cup points	NA	0.6 ± 1.5	0.4 ± 1.8	>0.96 (INTRA/ INTER)
Steppacher (2011)	25	Postoperative THA	2D-3D vs. 3D	APP, 6 rim points	NA	0.9 ± 2.8	1.7 ± 1.7	INCL = 0.96, AV = 0.95

APP = Anterior Pelvic Plane; THA = Total Hip Arthroplasty; INCL = Inclination; AV = Anteversion; COR = Center of Rotation; ICC = Intraclass Correlation Coefficient; 2D-3D = Registration aligning 2D radiographs to 3D models; CC = Craniocaudal direction; LM = Lateromedial direction; MoM = Metal-on-Metal implant; NA = Not Available.

4. Discussion

The findings of this literature review underscore the variability in methods used to assess the COR, AV and INCL, both in native and post-operative scenarios. The reviewed studies highlight various radiographic and 3D CT-based techniques, revealing different levels of reliability and accuracy, depending on the chosen measurement method and the reference standard used for validation. Although 2D X-ray methods remain widely used due to their accessibility and ease of use, their accuracy is inherently limited by the dimensional constraints of the modality. Standard radiographs capture only a 2D projection of 3D anatomy, making it difficult to fully account for spatial orientation and pelvic tilt. For example, the position of the COR can only be defined in two dimensions, and while INCL can be measured relatively consistently, AV requires estimating rotation in the transverse plane that is not directly visible on X-ray. These limitations affect both accuracy and reproducibility.

In terms of COR determination, X-ray-based methods showed high reliability, particularly the approach by Bjarnason et al. (10), which demonstrated near-perfect intra- and interobserver reliability (ICC values approaching 1). This suggests that traditional X-ray techniques can be highly consistent, especially when the anatomy is not severely altered. However, the study by Schofer et al. (11) demonstrated that more complex methods, such as those analyzing pelvic proportions and anatomical landmarks, could be necessary in cases with abnormal femoral head geometry.

For AV measurement, the review revealed significant variation in the X-ray based methods used, especially between those designed for native hips versus those used after THA. Studies by Özçelik et al. (16) showed that AV measurement in native hips using simple X-ray techniques can yield accurate results when compared to CT slices, although slight discrepancies (around 2.5°) were observed. The studies focusing on THA patients (such as those by Nho et al. (17), Lee et al. (18) and Alzohiry et al. (19)) demonstrated high reliability (ICC values over 0.9) across most methods, with the Lewinnek and Liaw methods showing small deviations from reference standards. Notably, only a limited number of studies reported detailed evaluations of INCL measurements. This may be due to the fact that INCL is generally more straightforward to assess on plain radiographs. As a result, there appears to be less emphasis in the literature on validating INCL compared to AV.

3D CT-based methods, by contrast, allow full spatial assessment of anatomical structures and consistently demonstrate superior precision across studies. Automated or semi-automated CT techniques using rim point placement and 3D reconstruction consistently achieved high ICCs (> 0.99) for AV and INCL, confirming their superior reproducibility. In comparative studies, 3D methods showed significant discrepancies with 2D measurements. However, these advantages must be weighed against the increased radiation exposure and resource requirements associated with CT imaging (45).

Between these two extremes, 2D-3D registration techniques present a promising hybrid approach. These methods use conventional X-rays in combination with CT-derived 3D models with some studies also incorporating statistical shape modeling to estimate 3D orientation from 2D images. In doing so, they not only improve the accuracy of 3D parameter estimation, but also reduce errors in 2D measurements by correcting for projection artifacts and differences in patient positioning. Multiple studies demonstrated minimal deviations from reference values for AV and INCL, which makes 2D-3D registration a promising approach combining the advantages of conventional radiographs with the accuracy of 3D imaging. These methods are particularly valuable in postoperative evaluations, offering a practical alternative to full 3D imaging.

A key limitation of this review is the variability in methodological approaches used, outcome measures and validation criteria, which hinders direct comparisons between studies. Moreover, while 2D-3D registration techniques show great promise, their implementation often relies on specific software, which may limit broader clinical adoption.

A specific consideration for this review is the applicability of these findings to patients with a LUMiC prosthesis. Most included studies were conducted in populations with conventional THAs, making it uncertain to what extent these results generalize to the LUMiC setting. The LUMiC implant differs substantially from standard cups, featuring a much larger volume of metal, which makes the radiographic contours of the cup more difficult to identify on 2D imaging. This increased radiodensity, combined with altered pelvic anatomy following tumor resection or complex revisions, may compromise the visibility of anatomical landmarks required for accurate measurement of acetabular AV and INCL.

5. Conclusion

This review provides a comprehensive overview of the current techniques for measuring COR, AV and INCL, both in native hips and post THA scenarios. The results indicate that while traditional 2D radiographic methods demonstrate reliability, advancements in 3D CT modeling offer superior accuracy and consistency. Therefore, the choice of a measurement method should be guided by the required level of accuracy. Integration of 2D-3D registration techniques may enhance reliability and accuracy in postoperative evaluations. However, it remains unclear to what extent these results can be translated to measurements in patients with a LUMiC prosthesis, given the implant's design and radiographic characteristics.

References

1. Jolles BM, Zangger P, Leyvraz PF. Factors predisposing to dislocation after primary total hip arthroplasty: A multivariate analysis. The Journal of Arthroplasty. 2002 Apr 1;17(3):282–8.

2. Bozic KJ, Kurtz SM, Lau E, Ong K, Vail TP, Berry DJ. The epidemiology of revision total hip arthroplasty in the United States. J Bone Joint Surg Am. 2009 Jan;91(1):128–33.

3. Sariali E, Klouche S, Mamoudy P. Investigation into three dimensional hip anatomy in anterior dislocation after THA. Influence of the position of the hip rotation centre. Clin Biomech (Bristol). 2012 Jul;27(6):562–7.

4. Lewinnek GE, Lewis JL, Tarr R, Compere CL, Zimmerman JR. Dislocations after total hip-replacement arthroplasties. JBJS. 1978 Mar;60(2):217.

5. Murphy WS, Yun HH, Hayden B, Kowal JH, Murphy SB. The Safe Zone Range for Cup Anteversion Is Narrower Than for Inclination in THA. Clin Orthop Relat Res. 2018 Feb;476(2):325–35.

6. D'Lima DD, Urquhart AG, Buehler KO, Walker RH, Colwell CW Jr. The effect of the orientation of the acetabular and femoral components on the range of motion of the hip at different head-neck ratios. J Bone Joint Surg Am. 2000 Mar;82(3):315–21.

7. Lum ZC, Dorr LD. Restoration of center of rotation and balance of THR. J Orthop. 2018 Dec;15(4):992–6.

8. Murray DW. The definition and measurement of acetabular orientation. The Journal of Bone & Joint Surgery British Volume. 1993 Mar 1;75-B(2):228–32.

9. Landis JR, Koch GG. The measurement of observer agreement for categorical data. Biometrics. 1977 Mar;33(1):159–74.

10. Bjarnason JA, Pripp AH, Reikeras O. Reliability of measures used in radiographic evaluation of the adult hip. Skeletal Radiology. 2015 Feb 20;44(7):935–9.

11. Schofer MD, Pressel T, Heyse TJ, Schmitt J, Boudriot U. Radiological determination of the anatomic hip centre from pelvic landmarks. Acta orthopaedica Belgica. 2010 Aug;76(4).

12. Fessy MH, N'Diaye A, Carret JP, Fischer LP. Locating the center of rotation of the hip. Surgical and Radiologic Anatomy. 1999 Jul;21(4):247–50.

13. John JF, Fisher PE. Radiographic determination of the anatomic hip joint center. A cadaver study. Acta Orthop Scand. 1994 Oct;65(5):509–10.

14. Pierchon F, Migaud H, Duquennoy A, Fontaine C. [Radiologic evaluation of the rotation center of the hip]. Revue de chirurgie orthopedique et reparatrice de l'appareil moteur. 1993;79(4).

15. Unger AS, Inglis AE, Ranawat CS, Johanson NA. Total hip arthroplasty in rheumatoid arthritis: A long-term follow-up study. The Journal of Arthroplasty. 1987 Jan 1;2(3):191–7.

16. Özçelik A, Akalın Y, Çalışır C, İnan U, Ömeroğlu H. Definition of a quantitative measurement method for acetabular version in a plain radiograph in the healthy adult hip. Eklem hastaliklari ve cerrahisi = Joint diseases & related surgery. 2015;26(1).

17. A simplified method to determine acetabular cup anteversion from plain radiographs. The Journal of Arthroplasty. 2004 Apr 1;19(3):387–90.

18. Radiographic calculation of anteversion in acetabular prostheses. The Journal of Arthroplasty. 1995 Jun

1;10(3):369–72.

19. Ackland MK, Bourne WB, Uhthoff HK. Anteversion of the acetabular cup. Measurement of angle after total hip replacement. J Bone Joint Surg Br. 1986 May;68(3):409–13.

20. Liaw CK, Hou SM, Yang RS, Wu TY, Fuh CS. A New Tool for Measuring Cup Orientation in Total Hip Arthroplasties from Plain Radiographs. Clinical Orthopaedics and Related Research®. 2006 Oct;451:134.

21. Pradhan R. Planar anteversion of the acetabular cup as determined from plain anteroposterior radiographs. J Bone Joint Surg Br. 1999 May;81(3):431–5.

22. McLaren RH. Prosthetic Hip Angulation1. Radiology. 1973 Jun 1;107(3):705–6.

23. Nho JH, Lee YK, Kim HJ, Ha YC, Suh YS, Koo KH. Reliability and validity of measuring version of the acetabular component. The Journal of Bone & Joint Surgery British Volume. 2012 Jan 1;94-B(1):32–6.

24. Lee GC, Lee SH, Kang SW, Park HS, Jo S. Accuracy of planar anteversion measurements using anteroposterior radiographs. BMC Musculoskeletal Disorders. 2019 Dec 5;20(1):1–8.

25. Alzohiry MA, Abdelnasser MK, Moustafa M, Mahran M, Bakr H, Khalifa Y, et al. Accuracy of plain antero-posterior radiographic-based methods for measurement of acetabular cup version. International Orthopaedics. 2018 Jun 4;42(12):2777–85.

26. Park YS, Shin WC, Lee SM, Kwak SH, Bae JY, Suh KT. The best method for evaluating anteversion of the acetabular component after total hip arthroplasty on plain radiographs. Journal of Orthopaedic Surgery and Research. 2018 Apr 2;13(1):1–8.

27. Nomura T, Naito M, Nakamura Y, Ida T, Kuroda D, Kobayashi T, et al. An analysis of the best method for evaluating anteversion of the acetabular component after total hip replacement on plain radiographs. The Bone & Joint Journal. 2014 May 1;96-B(5):597–603.

28. Marx A, von Knoch M, Pförtner J, Wiese M, Saxler G. Misinterpretation of cup anteversion in total hip arthroplasty using planar radiography. Archives of Orthopaedic and Trauma Surgery. 2006 Jun 21;126(7):487–92.

29. Shin WC, Lee SM, Lee KW, Cho HJ, Lee JS, Suh KT. The reliability and accuracy of measuring anteversion of the acetabular component on plain anteroposterior and lateral radiographs after total hip arthroplasty. The Bone & Joint Journal. 2015 May 1;97-B(5):611–6.

30. Manjunath KS, Soruban V, Gopalakrishna KG. Evaluation of radiological methods of assessing cup anteversion in total hip replacement. European Journal of Orthopaedic Surgery & Traumatology. 2015 Oct 10;25(8):1285–92.

31. Zhang H, Wang Y, Ai S, Chen X, Wang L, Dai K. Three-dimensional acetabular orientation measurement in a reliable coordinate system among one hundred Chinese. PLOS ONE. 2017 Feb 16;12(2):e0172297.

32. Chen X, Jia P, Wang Y, Zhang H, Wang L, Frangi AF, et al. A surface-based approach to determine key spatial parameters of the acetabulum in a standardized pelvic coordinate system. Medical Engineering & Physics. 2018 Feb;52:22–30.

33. Henckel J, Ramesh A, Hothi H, Richards R, Di Laura A, Hart A. The accuracy and precision of acetabular implant measurements from CT imaging. Front Bioeng Biotechnol. 2023 Apr 28;11:1150061.

34. Barlow KA, Krol Z, Skadlubowicz P, Dong C, Zivkovic V, Krieg AH. The “true” acetabular anteversion angle (AV angle): 2D CT versus 3D model. International Journal of Computer Assisted Radiology and Surgery. 2022 Jul 27;17(12):2337–47.

35. Park J, Kim JY, Kim HD, Kim YC, Seo A, Je M, et al. Analysis of acetabular orientation and femoral anteversion using images of three-dimensional reconstructed bone models. International Journal of Computer Assisted Radiology and Surgery. 2017 Jan 6;12(5):855–64.

36. Hart AJ, Dandachli W, Schlueter-Brust K, Henckel J, Cobb J. Large Ball Metal on Metal Hips Obscure Cup Angle Measurement on Plain Radiographs. HIP International. 2018 Jan 26;

37. Lu M, Zhou YX, Du H, Zhang J, Liu J. Reliability and Validity of Measuring Acetabular Component Orientation by Plain Anteroposterior Radiographs. Clinical Orthopaedics and Related Research®. 2013 Sep;471(9):2987.

38. Lubovsky O, Wright D, Hardisty M, Kiss A, Kreder H, Whyne C. Acetabular orientation: anatomical and functional measurement. International Journal of Computer Assisted Radiology and Surgery. 2011 Aug 7;7(2):233–40.

39. Nees TA, Mueller CT, Innmann MM, Spranz DM, Westhauser F, Renkawitz T, et al. Assessment Accuracy of 2D vs. 3D Imaging for Custom-Made Acetabular Implants in Revision Hip Arthroplasty. Journal of Personalized Medicine. 2024 Jul 30;14(8):808.

40. Craiovan B, Renkawitz T, Weber M, Grifka J, Nolte L, Zheng G. Is the acetabular cup orientation after total hip arthroplasty on a two dimension or three dimension model accurate? International Orthopaedics. 2014 Apr 16;38(10):2009–15.

41. Zheng G, Zhang X. Computer assisted determination of acetabular cup orientation using 2D-3D image registration. International journal of computer assisted radiology and surgery. 2010 Sep;5(5).

42. Weber M, Witzmann L, Wieding J, Grifka J, Renkawitz T, Craiovan B. Customized implants for acetabular Paprosky III defects may be positioned with high accuracy in revision hip arthroplasty. International Orthopaedics. 2018 Oct 10;43(10):2235–43.

43. Zheng G, von Recum J, Nolte LP, Grützner PA, Steppacher SD, Franke J. Validation of a statistical shape model-based 2D/3D reconstruction method for determination of cup orientation after THA. International Journal of Computer Assisted Radiology and Surgery. 2011 Jul 27;7(2):225–31.

44. Steppacher SD, Tannast M, Zheng G, Zhang X, Kowal J, Anderson SE, et al. Validation of a new method for determination of cup orientation in THA. Journal of Orthopaedic Research. 2009 Dec 1;27(12):1583–8.

45. de Gonzalez A B, Pasqual E, Veiga L. Epidemiological studies of CT scans and cancer risk: the state of the science. The British journal of radiology. 2021 Oct 1;94(1126).

Appendix

Pubmed search

504 results (October 9th, 2024)

("acetabular orientation"[tiab:~2] OR "bone anteversion"[mesh] OR "anteversion"[tiab] OR "center of rotation"[tiab] OR "inclination"[tiab] OR "acetabular version"[tiab:~2] OR "rotation centre"[tiab:~2] OR "joint centre"[tiab:~2] OR "rotation center"[tiab:~2] OR "joint center"[tiab:~2]) AND ("radiological determin*"[ti] OR "radiological diagnos*"[ti] OR "Tomography, X-Ray Computed"[Mesh] OR "CT"[ti] OR "Imaging, Three-Dimensional"[Majr] OR "Three-Dimensional"[ti] OR "3D imag*"[ti] OR "X-rays"[majr] OR "X ray*"[ti] OR "radiograph*"[ti] OR "radiography"[majr] OR "computed tomography"[ti] OR "computational modelling"[tiab]) AND ("Hip joint"[mesh] OR "hip joint*"[tiab] OR "total hip arthroplasty"[tiab] OR "Acetabul*"[tiab] OR "Acetabulum"[Mesh]) AND ("reliab*"[tiab] OR "validity"[tiab] OR "accur*"[tiab])